HHS Public Access

Author manuscript

Cancer Discov. Author manuscript; available in PMC 2021 November 01.

Published in final edited form as:

Cancer Discov. 2021 May ; 11(5): 1192–1211. doi:10.1158/2159-8290.CD-20-1243.

CRISPR Screening of CAR T Cells and Cancer Stem Cells Reveals Critical Dependencies for Cell-Based Therapies

Dongrui Wang[#1], **Briana C. Prager**[#2,3,4], **Ryan C. Gimple**[2,4,5], **Brenda Aguilar**[1], **Darya Alizadeh**[1], **Hongzhen Tang**[6,7,8], **Deguan Lv**[2,4], **Renate Starr**[1], **Alfonso Brito**[1], **Qiulian Wu**[2,4], **Leo J. Y. Kim**[2,4,5], **Zhixin Qiu**[2,4], **Peng Lin**[6,7,8], **Michael H. Lorenzini**[2,4], **Behnam Badie**[9], **Stephen J. Forman**[1], **Qi Xie**[6,7,8,§], **Christine E. Brown**[1,§,#], **Jeremy N. Rich**[2,4,10,§,#]

[1]T Cell Therapeutics Research Labs, Cellular Immunotherapy Center, Department of Hematology and Hematopoietic Cell Transplantation, City of Hope, Duarte, CA, 91010.

[2]Division of Regenerative Medicine, Department of Medicine, University of California, San Diego, San Diego, CA 92037.

[3]Cleveland Clinic Lerner College of Medicine at Cleveland Clinic & Case Western Reserve University, Cleveland, OH.

[4]Sanford Consortium for Regenerative Medicine, 2880 Torrey Pines Scenic Dr, La Jolla, CA 92037.

[5]Department of Pathology, Case Western Reserve University, Cleveland, OH.

[6]Key Laboratory of Growth Regulation and Translational Research of Zhejiang Province, School of Life Sciences, Westlake University, Hangzhou, Zhejiang, China.

[7]Westlake Laboratory of Life Sciences and Biomedicine, Hangzhou, Zhejiang, China.

[8]Institute of Basic Medical Sciences, Westlake Institute for Advanced Study, Hangzhou, Zhejiang Province, China.

[9]Division of Neurosurgery, Department of Surgery, City of Hope, Duarte, CA, 91010.

[10]Department of Neurosciences, University of California, San Diego, San Diego, CA 92037.

[#] These authors contributed equally to this work.

[§,]correspondence: Qi Xie: xieqi@westlake.edu.cn; Phone: 86-15501201789; Address: No.18 Shilongshan Road, Xihu District, Hangzhou, Zhejiang, China, 310004, Christine E. Brown: cbrown@coh.org; Phone: 626-256-4673; Address: 1500 E Duarte Road, Duarte, CA, USA, 91007, Jeremy N. Rich: drjeremyrich@gmail.com; Phone: 858-822-2703; Address: 9500 Gilman Drive #0695, La Jolla, CA, USA, 92093.

[#,]co-senior authors

Authors' Contributions

Conception and design: D. Wang, B.C. Prager, S.J. Forman, Q. Xie, C.E. Brown, J.N. Rich

Development of methodology: D. Wang, B.C. Prager, Q. Xie, C.E. Brown, J.N. Rich

Acquisition of data (provided animals, acquired patients, provided facilities, etc.): D. Wang, B.C. Prager, R.C. Gimple, B. Aguilar, H. Tang, D. Lyu, R. Starr, A. Brito, Q. Wu, P. Lin, B. Badie, Q. Xie

Analysis and interpretation of data (e.g. statistical analysis, biostatistics, computational analysis): D. Wang, B.C. Prager, D. Alizadeh, B. Aguilar, H. Tang, L. J. Y. Kim, Z. Qiu, Q. Xie, C.E. Brown, J.N. Rich

Writing, reviewing, and/or revision of the manuscript: D. Wang, B.C. Prager, D. Alizadeh, L. J. Y. Kim, Z. Qiu, P. Lin, S.J. Forman, Q. Xie, C.E. Brown, J.N. Rich

Administrative, technical, or material support (i.e., reporting or organizing data, constructing databases): S.J. Forman, C.E. Brown, J.N. Rich

Abstract

Glioblastoma (GBM) contains self-renewing GBM stem cells (GSCs) potentially amenable to immunologic targeting, but chimeric antigen receptor (CAR) T cell therapy has demonstrated limited clinical responses in GBM. Here, we interrogated molecular determinants of CAR-mediated GBM killing through whole-genome CRISPR screens in both CAR T cells and patient-derived GSCs. Screening of CAR T cells identified dependencies for effector functions, including TLE4 and IKZF2. Targeted knockout of these genes enhanced CAR antitumor efficacy. Bulk and single cell-RNA sequencing of edited CAR T cells revealed transcriptional profiles of superior effector function and inhibited exhaustion responses. Reciprocal screening of GSCs identified genes essential for susceptibility to CAR-mediated killing, including RELA and NPLOC4, the knockout of which altered tumor-immune signaling and increased responsiveness of CAR therapy. Overall, CRISPR screening of CAR T cells and GSCs discovered avenues for enhancing CAR therapeutic efficacy against GBM, with the potential to be extended to other solid tumors.

Keywords

T cell therapy; Glioblastoma stem cell; brain tumor

INTRODUCTION

Glioblastoma (GBM) ranks as one of the most lethal of human cancers with current therapy offering only palliation. Standard-of-care therapy consisting of maximal surgical resection followed by combined radiation and chemotherapy extends median survival by less than 3 months. The activation of anti-tumor immune responses may provide new opportunities to augment tumor control. As such, immunotherapies have been extensively investigated with positive results in preclinical studies, yet broad antitumor efficacy has not occurred in patients (1). The adoptive transfer of chimeric antigen receptor (CAR) engineered T cells has shown promising clinical activity in a subset of cancers, particularly B cell malignancies (2,3). To target GBM, CAR T cells have been engineered to recognize selected tumor antigens and have demonstrated cytolytic activity against GBM cells, including GBM stem cells (GSCs) (4–6). In patients with GBM, CAR T cell therapies have shown early evidence of activity, clinical feasibility, and safety (7–10). However, the overall outcomes of CAR T cell treatment remain unsatisfactory, prompting efforts to enhance the antitumor potency of GBM-targeting CAR T cells (11,12). The functional potentiation of CAR T cells, while attractive due to the modifiable nature of these cells, requires a comprehensive understanding of the molecular events regulating CAR T cell activation, exhaustion and tumor-induced immune suppression (11,13). Aside from CAR recognition of tumor antigens, the complicated and dynamic interaction between CAR T cells and their target tumor cells remains poorly characterized. Thus, there is a need for new strategies to further enhance CAR T cell potency.

Gene editing using the clustered randomly interspersed short palindromic repeats (CRISPR)-Cas9 is a promising approach to enhance cancer immunotherapy (14). Directed CRISPR-Cas9 gene knockout of checkpoint and other immune-regulatory receptors have shown utility for adoptive T cell therapy (15,16); however, this approach has focused on a limited

set of known pathways. By contrast, large CRISPR-knockout screens are an effective platform for unbiased target discovery and have been successfully used to identify genes in tumor cells which when deleted synergize with various types of immunotherapeutics (17–19). CRISPR screens in T cells identified modulators of TCR activation in response to stimulation with CD3/CD28 agonistic beads, viruses, or tumor cells (20–22). Although CAR constructs are synthetic TCR-like receptors incorporating CD3ζ and costimulatory domains, the molecular events are not identical between TCR and CAR T cell activation signaling pathways (23). Thus, unbiased CRISPR screen presents an attractive strategy for discovering key regulators of CAR-tumor interaction.

GSCs represent a potentially important cellular target in GBM, as they have been linked to therapeutic resistance, invasion into normal brain, promotion of angiogenesis, and immune modulation (24,25). We hypothesized that systematic interrogation of molecular regulation of CAR T cell efficacy against GBM could be optimized by screening both CAR T cells and GBM cells, thereby informing the interplay between a cell-based therapy and its target population. Here, we developed a robust method for performing whole-genome CRISPR-knockout screens in both GBM cells and human CAR T cells. Using our well-established CAR T cell platform targeting the tumor-associated surface marker interleukin-13 receptor α2 (IL13Rα2) (7,8,26), we identified novel CAR T cell- and tumor-intrinsic targets that substantially improved CAR T cell cytotoxicity against GSCs both *in vitro* and *in vivo*. Targeted genetic modification of identified hits in CAR T cells potentiated their long-term activation, cytolytic activity, and in vivo antitumor function against GSCs, demonstrating that CRISPR screen on CAR T cells leads to the discovery of key targets for augmenting CAR T cell therapeutic potency. In parallel, knockout of identified targets in GSCs sensitized them to CAR-mediated killing both in vitro and in vivo, revealing potential avenues for combinatorial inhibitor treatment to augment CAR T cell efficacy. Our findings represent a feasible and highly effective approach to discovering key targets that mediate effective tumor eradication using CAR T cells.

RESULTS

Genome-wide CRISPR screening of CAR T cells identifies essential regulators of effector activity

The fitness of CAR T cell products correlates with clinical responses (27,28), indicating that key regulators of CAR T cell function can be targeted to potentiate therapeutic efficacy. T cell exhaustion resulting from chronic tumor exposure limits CAR T cell antitumor responses (29). To identify the essential regulators of T cell functional activity in an unbiased manner, we performed genome-wide CRISPR screen adapting our previously developed in vitro tumor rechallenge assay, which differentiates CAR T cell potency in the setting of high tumor burden and reflects in vivo antitumor activity (30,31). IL13Rα2-targeted CAR T cells from two human healthy donors were lentivirally transduced to express the Brunello short-guide RNA (sgRNA) library (32) and the CAR construct, then electroporated with Cas9 protein. CAR T cells harboring CRISPR-mediated knockouts were recursively exposed to an excess amount of PBT030–2 GSCs (Fig. 1A), an IDH1 wild-type patient-derived GSC line that highly expresses IL13Rα2 (33). After tumor stimulation, CAR

T cells were sorted from co-culture and subsetted based on expression of the inhibitory receptor PD-1, which is associated with T cell exhaustion (Fig. 1A). To identify gene knockouts that augment CAR T antitumor activity, we identified sgRNAs enriched in the less exhausted PD1-negative versus PD1-positive CAR T cell compartments (Fig. 1B, Supplementary Fig. S1A and Supplementary Table 1). To eliminate targets that non-specifically impaired CAR T cell proliferation or viability, we excluded sgRNAs depleted (β-value < −1) in CAR T cells after 72-hour co-culture with GSCs or 72-hour monoculture (Fig. 1C). 220 genes were common hits in both T cell donors (Fig. 1D). Many of these 220 genes are induced by the IL4 receptor (IL4R), which suppresses T cell activity (34), as well as Type I Interferon, NFAT, TCF4, and JAK1/2, which all play complex roles on T cell activation and mediate T cell exhaustion and inhibition under some circumstances (35–38) (Fig. 1E). Additionally, these genes were enriched for pathways that contribute to T cell exhaustion, including nuclear receptor transcription and cholesterol responses (39,40) (Supplementary Fig. S1B). In contrast, genes preferentially depleted in PD1-positive cells included pathways associated with of T cell activation, including amide metabolism and NF-κB signaling (41,42), as well as negative regulation of oxidative stress-induced cell death (Fig. 1E). Together, this data verifies that our screen identified genes involved in T cell effector activity, providing candidate genes which can be modulated to prevent exhaustion and enhance effector function of CAR T cells.

CRISPR screening empowers discovery of targets that enhance CAR T cell cytotoxic potency

We interrogated the 220 targets enriched in PD1-negative cells common between two T cell donors (Supplementary Table 2), focusing on four representative genes identified in the top third of hits, which have not been previously explored for their role in enhancing CAR T cell function. These included the high-ranking hits: Eukaryotic Translation Initiation Factor 5A-1 (EIF5A), transcription factor Transducin Like Enhancer of Split 4 (TLE4), Ikaros Family Zinc Finger Protein 2 (IKZF2), and Transmembrane Protein 184B (TMEM184B) (Fig. 1F). Most sgRNAs targeting these genes (≥2 out of 4 in both replicates) were enriched in PD1-negative CAR T cells (Supplementary Fig. S1C). To verify the function of these targets by CRISPR-mediated KO on CAR T cells we leveraged the challenging in vitro killing assay (CAR:Tumor = 1:40), confirming that targeting TLE4, IKZF2, TMEM184B, or EIF5A improved *in vitro* killing potency of CAR T cells against GSCs, as well as the their expansion potential, although sgEIF5A-3 effects were more modest (Fig. 2A and B). Mechanistically, KO of these genes reduced PD-1 expression on CAR T cells following tumor stimulation (Supplementary Fig. S2A). We and others have shown that CAR T cell exhaustion is associated with co-expression of PD-1, LAG-3, and TIM-3 (43,44). All four KOs reduced CAR T cell exhaustion; TLE4- and IKZF2-KO most effectively (Fig. 2C). KO of these genes minimally affected initial CAR T cell activation upon tumor cell recognition (Supplementary Fig. S2B), suggesting that these KOs improved T cell fitness and long-term function instead of initial activation. Targeted KOs did not affect the expression and stability of the CAR in T cells (Supplementary Fig. S2C and D). As validation, we performed independent studies with a HER2-targeted CAR model that also demonstrated improvements in CAR killing and expansion, suggesting that genetic screens of CAR T cells may yield broadly effective molecular strategies (Supplementary Fig. S2E and F).

TLE4 is a transcriptional co-repressor of multiple genes encoding inflammatory cytokines (45) and IKZF2 is upregulated in exhausted T cells (37,46,47), supporting potential roles in inhibiting CAR T cell function. To elucidate molecular mechanisms underlying the regulation of CAR T cell activity, we compared the transcriptomes of CAR T cells with individual knockouts against cells transduced with non-targeted sgRNA (sgCONT). TLE4 KO in CAR T cells upregulated critical regulators of T cell activation, including the transcription factor EGR1, which promotes Th1 cell differentiation (48), and the metabolic regulator BCAT, which mediates metabolic fitness in activated T cells (49) (Supplementary Fig. S2G). IKZF2 KO in CAR T cells upregulated proinflammatory cytokines and pathways, including CXCL8, CCL3, and CCL4 (50–52), as well as EGR1, similar to TLE4 KO (Supplementary Fig. S2H). We next compared transcriptional profiles of TLE4 or IKZF2 KO CAR T cells to the signatures of known T cell subsets and pathways (35,53,54). TLE4 or IKZF2 KO induced molecular signatures representing activation over memory T cells, together with key T cell activation signaling pathways (TCR signaling, T cell activation, AP-1, and ZAP) (Fig. 2D and E; Supplementary Fig. S2I and S2J). T cell activation characteristics in TLE4-KO or IKZF2-KO cells were uncoupled from exhaustion (Fig. 2D and E), suggesting retention of CAR T cell function. TLE4-KO cells downregulated an apoptosis signature (Fig. 2D and F) and upregulated AP-1 signaling, which maintains CAR T cell function (55) (Fig. 2G). In particular, the AP-1 family transcription factor FOS was enriched after TLE4 KO, together with many of its downstream targets (Fig. 2G). As overexpression of the AP-1 family member JUN prevents CAR T cell exhaustion (55), we investigated whether TLE4 KO phenocopied transcriptional changes of JUN overexpression, revealing that genes upregulated with TLE4 KO overlapped with genes with upregulated following JUN overexpression (Fig. 2H). IKZF2 KO upregulated pathways involving interactions between cytokines and their receptors, as well as NFAT signaling, which regulates key molecular signals following T cell activation (56) (Fig. 2I and J). As EGR1 was upregulated after IKZF2 KO, many genes in these pathways were likely downstream targets (Fig. 2I and J).

Whole-transcriptome analyses following TMEM184B or EIF5A KO revealed convergence of altered pathways, similar to those induced by TLE4 or IKZF2 KO, including the upregulation of BCAT1, EGR1, and IL17RB (Supplementary Fig. S3A and S3B) and the acquisition of memory or effector over naïve T cell signatures (Supplementary Fig. S3C and S3D). However, targeting TMEM184B or EIF5A did not enrich for cytokine secretion and response pathways in CAR T cells (Supplementary Fig. S3E and S3F), which were found in TLE4-KO or IKZF2-KO CAR T cells. As these cytokines (CCL3 and CCL4) maintain T cell function during chronic viral infection and in the tumor microenvironment (57,58), our results indicate that TMEM184B-KO and EIF5A-KO CAR T cells might be prone to terminal effector differentiation and subsequent exhaustion, thereby compromising their overall functional capability despite their potent in vitro cytotoxicity. Overall, knockout of these genes in CAR T cells also maintained transcriptional profiles of T cell activation, which are associated with effector potency.

Targeting TLE4 and IKZF2 modify CAR T subsets associated with effector potency

To determine the impact of TLE4 or IKZF2 KO on specific subpopulations of CAR T cells, we performed comparative single-cell RNA-sequencing (scRNAseq) on KO and control CAR T cells with or without stimulation by tumor cells. Comparing TLE4-KO cells with control CAR T cells by unbiased clustering of pooled data identified 10 different clusters, the distribution of which was greatly influenced by stimulation (Fig. 3A-C; Supplementary Fig. S4A). CD4+ and CD8+ CAR T cells were well delineated (Supplementary Fig. S4B). Stimulated cells downregulated naïve/memory-related markers (e.g. IL7R and CCR7) and upregulated activation-related markers (e.g. MKI67 and GZMB) (Supplementary Fig. S4C). Stimulation enriched clusters 0, 1, 4, and 10 (showing high expression of activation or exhaustion markers) and depleted clusters 3, 5, 7, and 9 (expressing naïve/memory markers) (Fig. 3D). TLE4 KO minimally impacted the overall distribution of unstimulated CAR T cells; however, cluster 8 was depleted after stimulation only in control, but not in TLE4-KO cells (Fig. 3C and D). This cluster represented a subset of CD4+ T cells expressing multiple costimulatory molecules, including CD28, ICOS, CD86, and TNFRSF4 (OX40), as well as the cytokine IL-2 (Fig. 3D; Supplementary Fig. S4D). Although no proliferative activity was detected in this cluster (indicated by low Ki67), preservation of this cluster in TLE4-KO cells was maintained post-stimulation (Fig. 3D). In TLE4-KO cells, cluster 8 also showed expression of the immune stimulatory cytokine CCL3 (Fig. 3E), costimulatory molecule TNFRSF4 (Fig. 3F), and AP-1 transcription factors FOS and JUN (Supplementary Fig. S4E and S4F), which were minimally expressed in control cells. Cluster 10 was an activated CD4+ subset expressing multiple cytokines, including IL-2 and TNF, and this cluster displayed greater post-stimulation expansion in TLE4-KO cells (Fig. 3D). In the clusters with activation signatures (0, 1, and 10), TLE4 KO upregulated IFNG, BCAT, GZMB, CCL3, and CCL4 (Fig. 3G and H; Supplementary Fig. S4G-I). Combining the transcriptome readouts from all single cells revealed that tumor stimulation in TLE4-KO cells induced T cell stimulatory and cytotoxic factors (e.g. GZMB, CCL3, CCL4, and IFNG) to a greater degree than control CAR T cells (Supplementary Fig. S4J). Taken together, the enhanced cytotoxicity of TLE-KO CAR T cells could result from the preservation of specific T cell subsets after tumor stimulation.

Comparison between IKZF2-KO cells and control CAR T cells identified 10 clusters using unbiased clustering of pooled data (Fig. 4A). In parallel with the comparisons between TLE4-KO vs. control cells, we observed a dramatic change in cluster distribution and gene expression after stimulation, with moderate changes from IKZF2 KO (Fig. 4B and C; Supplementary Fig. S5A-D). Given a role for IKZF2 in regulatory T cells (Treg) (59), cluster 0, characterized by Treg signatures (e.g. CLTA4, FOXP3 and IL2RA), was reduced in IKZF2-KO cells (Fig. 4B-D). Cluster 10 was induced after stimulation, enriched in IKZF2-KO cells, and expressed elevated levels of AP-1 signaling molecule FOS and JUN (Fig. 4B-D). These cells expressed a limited repertoire of cytokines beyond TNF, but had medium-to-high levels of Ki67, high expression of EGR1 and IL2, and exclusively expressed CXCL10 and CCND1 (Fig. 4D-F; Supplementary Fig. S5D). Upregulated genes in cluster 10 were enriched for transcriptional regulation by ATF3 and JUN (Supplementary Fig. S5E and F). This subset contained a very limited number of cells and was only present upon stimulation, potentially explaining the lack of differential expression of FOS

and JUN in bulk RNA-seq analysis in IKZF2-KO cells. Cluster 2 was also expanded after stimulation in both IKZF2-KO and control cells (Fig. 4D; Supplementary Fig. S5A). However, induction of activation-associated genes in this cluster, including IFNG, CCL3, and CCL4, was more robust in IKZF2-KO vs. control cells upon tumor stimulation (Fig. 4G and H; Supplementary Fig. S5G). In IKZF2-KO cells, CCL3 was expressed at higher levels in clusters 0, 1, and 9 (Fig. 4G). As a result, IKZF2-KO cells exhibited an augmented responsiveness to tumor stimulation, illustrated by the upregulation of activation-associated cytokines (Supplementary Fig. S5H). Overall, scRNAseq analysis revealed that TLE4 or IKZF2 KO resulted in the preservation or expansion of certain CAR T cell subset after tumor stimulation. These cellular subsets displayed transcriptional signatures of T cell cytotoxicity and/or immune stimulation, providing some underlying mechanisms of their superior effector function against tumor cells.

Genome-wide screening of GSCs identified genes mediating resistance to CAR T cells

Augmenting efficacy of CAR T cells against GBM can be approached by studying T cells themselves, as above, which may inform targeted KOs in addition to CAR engineering for enhancing CAR activity. Reciprocal screening of GBM cells, especially GSCs, potentially informs interactions with CAR T cells to predict clinical responsiveness to CAR T cell therapy. To identify potential genes in GSCs that promote resistance to CAR-mediated cytotoxicity, we performed genome-wide CRISPR screens on two independent patient-derived GSC lines (PBT030–2 and PBT036), both derived from primary GBM tumors with high expression of IL13Rα2 (33). To identify tumor cell targets that rendered GBM cells more susceptible to T cell immunotherapy, we subjected GSCs to two rounds of co-culture with IL13Rα2-targeted CAR T cells (Fig. 5A and Supplementary Fig. S6A). We identified sgRNAs that were enriched (β-value > 1) or depleted (β-value < −1) in the surviving GSCs compared with GSCs in monoculture for the same amount of time (Fig. 5B). The genes with sgRNAs depleted in co-culture (β-value < −1) represented targets that promoted CAR killing upon knockout (Fig. 5C). To exclude sgRNAs that non-specifically targeted essential genes for GSC survival, we removed gene hits that were depleted in GSCs after 48-hour culture without CAR T cells (Fig. 5C). A total of 159 CAR-modulating genes were identified as hits in either GSC line, with only 4 overlapping targets common to both lines (Fig. 5D). Enriched pathways included tumor immune modulation, such as MHC I antigen presentation, IL-1 signaling and NF-κB activation (Fig. 5E), indicating that sgRNAs depleted in surviving GSCs targeted genes responsible for resistance to T cell killing.

Knockout of RELA or NPLOC4 sensitizes GSCs to CAR-mediated antitumor activity

Next, we sought to confirm and further characterize the function of common top hits whose deletion promoted CAR killing (Fig. 5D). V-Rel Reticuloendotheliosis Viral Oncogene Homolog A (RELA) and Nuclear Protein Localization Protein 4 Homolog (NPLOC4) were selected for further validation as all sgRNAs targeting these two genes in the screen showed depletion in GSCs co-cultured with CAR (Fig. 5F). As expected from our selection process, CRISPR-mediated Knockout (KO) of either RELA or NPLOC4 caused limited reduction in the growth of GSCs *in vitro* compared with GSCs transduced with control non-targeted sgRNAs (sgCONT) (Supplementary Fig. S6B). When co-cultured with CAR T cells in a challenging *in vitro* model at low T cell ratios (E:T=1:40; 48hr), RELA or NPLOC4 KO

in GSCs increased susceptibility to CAR T cell-mediated killing (Fig. 6A), which was also associated with increased expansion of CAR T cells (Fig. 6B). Thus, knockout of either RELA or NPLOC4 in GSCs enhanced the cytotoxic and proliferative potency of CAR T cells.

RELA (also known as p65) is an NF-κB subunit that regulates critical downstream effectors of immunosuppressive pathways in tumors (60,61). NPLOC4 mediates nuclear pore transport of proteins, but its role in cancer or immune modulation remains unclear. To elucidate the mechanism by which these genes mediate GSC sensitivity to CAR T cell killing, we performed in-depth characterization of GSCs harboring knockout of each gene. The increased sensitivity was not a result of alterations in target antigen expression on GSCs (Supplementary Fig. S6C). CAR T cells induced PD-L1 in GSCs, which was not altered by depletion of either RELA or NPLOC4 (Supplementary Fig. S6D). Likewise, CAR T cells co-cultured with GSCs transduced with sgCONT, sgRELA, or sgNPLOC4 did not show differences in activation after stimulation as indicated by markers CD69 and CD137, or exhaustion measured by levels of exhaustion markers, including PD-1, LAG-3, and TIM-3 (30) (Supplementary Fig. S6E). Whole-transcriptome analysis of GSCs after RELA KO showed downregulation of immunosuppressive cytokines, including CXCL3, CCL20, and IL-32 (Fig. 6C), all of which suppress antitumor immune responses (62,63). Downregulated genes were highly enriched for known direct transcriptional targets of RELA, and RELA KO reduced NF-κB signaling, as well as the immunosuppressive effectors of TNF responsiveness and IL-10 signaling (Fig. 6D and E; Supplementary Fig. S6F). Targeting NPLOC4 in GSCs downregulated genes mediating rearrangement of extracellular matrix (ECM), including proteoglycans, integrins and collagens (Fig. 6F-H). Reactome analysis revealed the involvement of specific tumorigenic factors, such as EGFR and PDGFA (Fig. 6G). Pathways downregulated after NPLOC4 depletion were highly enriched for ECM remodeling and cell adhesion (Fig. 6H and Supplementary Fig. S6G). Although tumor ECM remodeling has been reported to suppress antitumor immune responses by preventing T cell trafficking into the tumors, ECM-associated factors may directly repress T cell activity (64,65). To interrogate NPLOC4 interactions, we performed immune-precipitation followed by mass spectrometry (IP/MS), revealing that NPLOC4 bound multiple targets in immune-related pathways (IL-1, Fc receptor, antigen presentation), Wnt signaling, and protein synthesis/degradation pathways (Supplementary Fig. S7A). These mechanisms may regulate the immune-related profiles of GSCs, where NPLOC4-KO led to the upregulation of immune stimulatory cytokines (Supplementary Fig. S7B and C). Together, we found that tumor-intrinsic regulators RELA and NPLOC4 mediate GBM resistance to CAR T cell cytotoxicity via mechanisms distinct from induction of CAR T cell exhaustion.

CRISPR screening identified targets with functional and clinical relevance in GSCs

Next, we used an orthotopic intracranial patient-derived xenograft model to evaluate whether modulating the identified targets on GSCs enhanced the antitumor function of CAR T cells in a preclinical setting. Established GBM PDXs were treated with CAR T cells delivered intracranially into the tumors, mimicking our clinical trial design of CAR T cell administration to patients with GBMs (7,66). First, we used CAR T cells without CRISPR knockout to treat control, RELA-KO, or NPLOC4-KO tumors. A limited number

of CAR T cells (50,000/mouse) completely eradicated xenografts derived from RELA-KO or NPLOC4-KO GSCs, whereas the same CAR T cells were only partially effective against tumors established with sgCONT-GSCs (Fig. 7A and B; Supplementary Fig. S8). These results suggest that tumors with low expression of RELA and/or NPLOC4 are more sensitive to CAR T therapy.

To further dissect the roles of RELA and NPLOC4 in immune modulation in GBM, we analyzed 41 GSC samples, and found that high RELA- or NPLOC4-expressing GSCs showed enrichment in immune-suppression signatures (Supplementary Fig. S9A and B). Interrogating the Cancer Genome Atlas (TCGA) GBM dataset revealed that RELA and NPLOC4 both positively correlated with TGF-β signaling, a key pathway mediating immune suppression in GBMs and many other types of tumors (67). RELA was also positively correlated with immunosuppressive regulatory T cell signatures and negatively correlated with the signatures of antitumor T cell responses (lymphocyte infiltration, TCR richness, Th1 and CD8 T cells) (Fig. 7C). NPLOC4 was negatively correlated with the immune stimulatory IFNγ responses (Fig. 7D). The infiltration signature of CD4+ and CD8+ T cells in GBM inversely correlated with RELA or NPLOC4 expression (Supplementary Fig. S9C and D). These results suggest that high expression of RELA and NPLOC4 in GBM are indicative of a more suppressive tumor immune microenvironment, and, repressed antitumor T cell responses.

CRISPR screening identified targets with functional and clinical relevance in CAR T cells

We next evaluated the molecular targets identified in our CAR T cell screen in vivo, with the goal of establishing clinically translatable strategies to improve CAR T cell function. The antitumor function of different CAR T cells were tested against tumors without CRISPR knockouts, with a further limited CAR T cell dose (20,000/mouse) showing enhanced survival benefit as compared to the control CAR T cells failed to achieve long-term tumor eradication (Fig. 7E and F). Consistent with improved maintenance of T cell effector activity and decreased exhaustion, targeting either TLE4 or IKZF2 augmented in vivo antitumor activity of CAR T cells against PDXs, as measured by extension of survival in tumor-bearing mice (Fig. 7E and F; Supplementary Fig. S10). Depletion of TMEM184B or EIF5A in CAR T cells showed a trend towards improved efficacy in increasing the survival of tumor-bearing mice (Supplementary Fig. S11A and B). Therefore, these targets on GSCs and CAR T cells can be exploited to advance the efficacy of CAR therapy against established GBM tumors.

We then investigated whether the CAR T cell targets indicate the potency of clinical therapeutic products. We then mapped upregulated genes in IKZF2-KO CAR T cells compared to control CAR T cells after tumor stimulation, with the transcriptomes of CAR T cell products from patients with chronic lymphocytic leukemia (CLL) achieving complete responses (CR) or no responses (NR) (27). Supporting our results, these genes were induced to a greater degree after CAR stimulation in the products from patients achieving CR (Fig. 7G). Similarly, genes enriched in cluster 10, whose expansion was induced by tumor stimulation and further augmented with TLE4 KO, were also highly expressed in the products from patients with CR (Fig. 7H). Further, both TLE4- and IKZF2-KO led to gene

upregulation similar to comparisons of products from patients with CR and NR (Fig. 7I and J).

To further understand how TLE4 and IKZF2 contribute to the function of clinical CAR T cell products, we analyzed scRNAseq from 24 patient-derived CD19-CAR T cell products (68). An unbiased clustering of the scRNAseq data revealed that IKZF2 expression was highly enriched in cluster 7 (Supplementary Fig. S12A and B), overlapping with key markers of immune-suppressive Tregs (CTLA4, FOXP3, IL2RA; Supplementary Fig. S12C and D). Cluster 7 was more frequently detected in patients with progressive disease (PD) than those with complete responses (CR) (Supplementary Fig. S12E). In these same cells, cluster 11 represented exhausted T cells, as indicated by the markers TOX and TOX2 (Supplementary Fig. S13A-C) (37). This cluster showed low expression of TLE4-repressed genes, indicating high TLE4 activity (Supplementary Fig. S13D and E). Further, TLE4 was upregulated in CAR T cells undergoing extended ex vivo culture (Supplementary Fig. S13F), a process associated with impaired effector function (69). Together, these observations establish that the targets identified from CRISPR screening have clinical implications for both tumor immunoreactivity and CAR T cell functional potency (Supplementary Fig. S14).

DISCUSSION

T cell-based therapies may offer several advantages in GBM therapy. T cell-based therapies, especially when delivered into the cerebrospinal fluid (CSF), traffic to multifocal tumor populations within the central nervous system (CNS) (8,70–72), thus overcoming challenges associated with the blood-brain barrier that limits the CNS penetration of most pharmacologic agents. T cell therapies compensate for cellular plasticity within brain tumors more effectively than traditional pharmacologic agents. GBMs display striking intratumoral heterogeneity, and tumor cells readily compensate for targeted agents against specific molecular targets. With T cell therapy targeting different antigens, personalized treatments based on the antigen expression profile of individual tumors may be designed. T cell-based therapies induce secondary responses that augment endogenous anti-tumor responses. Adoptive cell transfer, especially CAR T therapies, have been investigated in clinical trials for GBM patients, but efficacy has been restricted to limited cases (11). Our focus on CAR T cells was prompted not only by the potential value for clinical translation, but also as our findings inform a broader understanding of T cell function in brain tumor biology.

Previous genetic screens used to identify interactions between immune cells and tumor cells have largely focused on the tumor cells (18,19,29), as these cells are easier to manipulate genetically. Screens on tumor-reactive mouse T cells have also been reported (20,73,74) given the establishment of Cas9-knockin mouse strain (75), as well as the convenience to acquire large numbers of these cells. Here, we interrogated both the human CAR T cell and tumor cell compartments. The screening strategy on CAR T cells was greatly facilitated by the development of the non-viral Cas9 expression system in primary human T cells (21). Here, the screening on tumor cells was performed on two independent GSCs, displaying a relatively narrow range of shared molecular targets involved in mediating responses to CAR

T cells in our studies, which might be a consequence of subtype difference between these GSC lines (33). The screening identified both rational targets (RELA/p65) and novel targets (NPLOC4) in immune regulation, which were not restricted to a specific GBM molecular subclass. NPLOC4 displayed unexpected associations with GBM-targeting immune cell activity, as NPLOC4-KO in GSCs led to enhanced potency of CAR T cells and increased cytokine production in GSCs, although the detailed mechanism awaits further investigation. In the analyses of GSC models and TCGA database, high RELA and NPLOC4 expression was associated with immuno-suppressive signatures. More specifically, higher expression of RELA and NPLOC4 in GBMs correlated with low infiltration of both CD4+ and CD8+ T cells, indicating that targeting these genes may confer immune modulatory effect and enhance antitumor T cell responses in GBMs.

The assay used for CRISPR screening in T cells is crucial for reliable readouts and is required for its sensitivity to differentiate effective versus non-effective therapies. Although the in vivo antitumor efficacy in mouse models has been the standard to evaluate the functional quality of T cells in adoptive transfer, the utilization of this system in screening has been controversial. Tumor-infiltrating T cells harvested after the injection of therapeutic cells display signatures of tumor reactivity (73) or, conversely, T cell exhaustion (40). The differential results appear model dependent, leading to mixed interpretation of the results. The co-culture assays that we used in this study identified key regulators by creating challenging screening environments. For the screening on GSCs, two rounds of short-term (24 h) killing with relatively large number of T cells (total E:T = 1:1) was performed and GSCs were harvested immediately after the second round of killing, minimizing the effect of knocking out genes essential for the GSC growth. For the screening on CAR T cells, a repetitive challenge assay was used with excessive number of GSCs (total E:T = 1:12), which we have shown to induce CAR T cell exhaustion (30). The screen was performed by comparing a less exhausted (PD1-negative) with a more exhausted (PD1-positive) subset, informing prioritization for maintenance of recursive killing function, while reducing the noise from tumor cell or T cell growth. The screening was performed with two independent CAR T cell donors, and the relatively small proportion of overlapping hits between the two donors was expected and consistent with previous studies (21,76), due to the variation in T cell populations between individuals. The target validation was done with different T cell donors and CAR platforms; therefore, the discovered immunotherapy targets may be generalizable to multiple CAR designs. While we validated 4 representative genes, the screening on CAR T cells resulted in over 200 potential targets involved in critical pathways of T cell biology and activation, offering additional targets for future investigation of CAR refinement. One limitation of our approach, however, is the exclusion of apoptosis pathways in tumor cells due to its critical role in tumor cell growth, which have been demonstrated as important regulators of CAR T cell-mediated tumor killing as well as tumor-induced CAR T cell exhaustion (29).

T cell exhaustion has been considered as one of the major hurdles for reducing CAR T cell potency (77–79). Blocking/knockout of inhibitory receptors is being rigorously investigated to augment CAR activity or other tumor targeting T cells (29,80,81). T cell exhaustion is a feedback mechanism after activation, occurring upon recursive exposure to antigens in the contexts of chronic infection or the tumor microenvironment (78,82). compromising their

antitumor potency (79). Here, we observed that TLE4 or IKZF2 KO resulted in unstimulated CAR T cells to express transcriptional profiles of activation, while prohibiting exhaustion. AP-1 family transcription factors FOS and JUN, which were induced after both TLE4- and IKZF2-KO, provide a possible mechanism by which CAR T cell fitness was protected. The protein c-Jun forms homodimers or c-Fos/c-Jun heterodimers to initiate transcription of proinflammatory cytokines, and heterodimers with other co-factors (including BATF, IRF4, JUNB, and JUND) induce inhibitory receptors or suppress transcriptional activity of c-Jun (83–86). FOS was more upregulated than suppressive co-factors after TLE4-KO; therefore, driving T cell activation together with a protection from exhaustion, which was reminiscent of the effect after expressing c-Jun in CAR T cells with tonic signaling (55). In IKZF2-KO cells, however, the uncoupling of activation from exhaustion signatures was likely influenced by the upregulation of cytokines CCL3 and CCL4, which inversely correlated with PD-1 expression during T cell exhaustion (87). Both TLE4 or IKZF2 KO in CAR T cells upregulated essential regulators for Th1 cell differentiation (BCAT and EGR1, respectively), consistent with a previously identified role of this T cells population in mediating antitumor immunity (88,89). Consequently, targeted KOs in CAR T cells enhanced not only killing, but also expansion potential, which is correlated with clinical responses (90). Although it remains unresolved if these KOs potentiate CAR activity in immune-competent settings, our results have revealed the feasibility that CAR T cells can be modified for their activation/exhaustion signals to achieve functional improvement in clinically-relevant models. Consistent with these findings, we explored public databases of scRNAseq on patient-derived CAR T cell products and discovered that high IKZF2 expression and TLE4 activity were associated with other suppressive/exhaustion signatures of CAR T cells as well as poor clinical responses.

Single cell analyses reveal subset composition within a mixed cell sample, such as CAR T cells, in which minority populations serve critical roles. scRNAseq revealed that CAR activation, rather than genetic modification of CAR T cells (TLE4 or IKZF2 KO), resulted in a major cluster switch, which is consistent with the observation that TLE or IKZF2 KO in monoculture CAR T cells did not dramatically alter transcriptional profiles, as suggested by bulk RNA-seq. Following tumor challenge, knockout of targeted genes upregulated T cell activation markers and proinflammatory cytokines across different clusters, especially IFNG and CCL3, which showed similar induction by both TLE-KO and IKZF2-KO. Further, after CAR activation, TLE4 KO maintained a specific cluster, which existed pre-activation, and IKZF2 KO led to the emergence of a new cluster. The transcriptional signature of these clusters (expression of several costimulation molecules and cytokines) indicated their critical role in mediating effector function of CAR T cells. Therefore, the superior functions of TLE4-KO or IKZF2-KO CAR T cells were likely the result of a generally elevated activation state, as well as the stimulatory effect from critical subsets. Our scRNAseq results also suggested the existence of Treg-like populations, the expansion of which was seen after CAR activation and can be reduced by IKZF2-KO. The suppressive function of these cells still requires further investigation, but these results indicate the potential of enhancing CAR function through inhibiting differentiation towards Treg-like cells. Both TLE4-KO and IKZF2-KO CAR T cells appear to modify specific CD4+ T cell subsets, which supports our

previous observation that CD4+ CAR T cells play a critical role in mediating potent effector function (30).

In summary, whole-genome CRISPR knockout screens identified a limited set of key targets on GSCs that promote resistance to CAR killing. Modifying these genes before CAR T cell infusions, with genetic or chemical approaches, might be a potential strategy to enhance CAR T cell antitumor function and also guide patient selection. The spectrum of identified CAR T targets in our screen was broad, but manipulating expression of several of these targets appeared to regulate shared transcriptional programs, including cytokines and AP-1 regulation. Given the exciting advances in CAR T engineering with logic gates, it should be possible to interrogate multiple molecular targets within CAR T cells to determine potential synergy or additional benefit. Although our screens and evaluations were mainly focused on GSCs, the results are also expected to be consistent non-GSC populations, as CAR-mediated cytotoxicity has been demonstrated not to bias between antigen-positive GSCs and more differentiated tumor cells (4–6). While further investigation is needed to demonstrate the function of these targets in T cells harboring other CAR constructs, our results found that most of the targets selected for deeper studies regulate core pathways in immune cell function, suggesting that these targets likely have broad regulatory function in immune cell antitumor function in various contexts. Future studies will also permit interrogation of critical targets in an immune-intact environment, but our current focus was to interrogate molecular regulators directly involved in CAR T killing of the therapeutically resistant human GSC population. Overall, the bidirectional screening provides a platform to robustly identify targets with the potential towards clinical benefit in CAR T and other adoptive cell transfer therapies.

METHODS

Lentiviral transduction on GSCs

GSCs were acquired from patient specimens at City of Hope under protocols approved by the IRB, and maintained as tumorspheres in GSC media as previously described (4,91). GSC lines used in this study to test CAR T cell function are IDH1/2-wildtype. The sgRNA library and single-targeted sgRNA lentiviral plasmids (containing a puromycin-resistance gene) for GSC transduction were purchased from Addgene (#73179 and #52961, respectively). Lentiviral particles were generated as previously described (92). For lentiviral transduction, GSC tumorspheres were dissociated into single cells using Accutase (Innovative Cell Technologies), resuspended in GSC media and lentivirus was added at a 1:50 v/v ratio. GSCs were then washed once after 12 hours, resuspended in fresh GSC media and cultured for 3 days. To ensure that only transduced cells were expanded for further assays, GSCs were selected by puromycin (Thermo Fisher Scientific) for 7 continuous days, with a 1:10000 v/v ratio into GSC media.

Lentiviral transduction on primary human T cells

Naïve and memory T cells were isolated from healthy donors at City of Hope under protocols approved by the IRB (26,30). The constructs of IL13Rα2-targeted and HER2-targeted CARs were described in previous studies (8,26,93). Procedures of CAR-only

transduction on primary human T cells were previously described (44). The sgRNA library and single-targeted sgRNA lentiviral plasmids for T cell transduction were purchased from Addgene (#73179 and #52961, respectively). All sgRNA plasmids contain a puromycin-resistance gene. Dual transduction of CAR and sgRNA were performed using modification of previously reported procedures (21). In brief, primary T cells were stimulated with Dynabeads Human T expander CD3/CD28 (Invitrogen) (T cells: beads = 1:2) for 24 hours and transduced with sgRNA lentivirus (1:250 v/v ratio). Cells were washed after 6 hours and then transduced with CAR lentivirus (multiplicity of infection [MOI] = 0.5). 4 days after CAR transduction, CD3/CD28 beads were removed and cells were resuspended in Lonza electroporation buffer P3 (Lonza, #V4XP-3032) (2×10^8 cells/mL). Cas9 protein (MacroLab, Berkeley, 40mM stock) was then added to the cell suspension (1:10 v/v ratio) and electroporation was performed using a 4D-Nucleofactor™ Core Unit (Lonza, #AAF-1002B). Cells were recovered in pre-warmed X-VIVO 15 media (Lonza) for 30 min before proceeding to ex vivo expansion. All T cell transduction and ex vivo expansion experiments were performed in X-VIVO 15 containing 10% FBS, 50 U/ml recombinant human IL-2 (rhIL-2), and 0.5 ng/ml rhIL-15, at 6×10^5 cells/ml. To ensure that only sgRNA-transduced cells were expanded, puromycin (1:10000 v/v ratio) was added to the media 3 days after electroporation, and puromycin selection was performed for 6 continuous days before CAR T cells were used for further assays. CRISPR screening was performed on two independent donors, and other 2 donors are used to generate IL13Rα2-targeted and HER2-targeted CARs, respectively.

CRISPR screening on GSCs

GSCs transduced with the CRISPR KO library were dissociated into single cells, and co-cultured with CAR T cells at an effector: target ratio of 1:2 in culture plates pre-coated with matrigel. After 24 hours, the media containing CAR T cells and tumor debris were removed, and same number of CAR T cells were added in fresh media. 24 hours after the second CAR T cell addition, the media were removed and remaining GSCs were washed with PBS and harvested. Genomic DNA was isolated from the remaining GSCs after co-culture with CAR T cells, as well as GSCs harvested before co-culture and GSCs after monoculture for 48 hours.

CRISPR screening on CAR T cells

T cells transduced with CAR and the CRISPR KO library were co-cultured with GSC at an effector: target ratio of 1:4 in culture plates pre-coated with matrigel. After 48 hours, CAR T cells were re-challenged by GSCs doubling the number of the initial co-culture. 24 hours after the rechallenge, the co-culture was harvested and stained with fluorescence-conjugated antibodies against human CD45 (BD Biosciences Cat# 340665, RRID:AB_400075), PD1 (BioLegend Cat# 329922, RRID:AB_10933429) and IL13 (BioLegend Cat# 501914, RRID:AB_2616746). Different subsets were sorted using an Aria SORP (BD Biosciences): total CAR T cells (CD45+, IL13+), PD1+ CAR T cells (CD45+, IL13+, PD1+) and PD1- CAR T cells (CD45+, IL13+, PD1-). Genomic DNA was isolated from the sorted subsets of cells, as well as CAR T cells harvested before co-culture and CAR T cells after monoculture for 72 hours.

CRISPR-Cas9 screen analysis

FASTQ files were trimmed to 20 bp CRISPR guide sequences using BBDuk from the BBMap (https://jgi.doe.gov/data-and-tools/bbtools) (RRID:SCR_016965) toolkit and quality control as performed using FastQC (RRID:SCR_014583, https://www.bioinformatics.babraha-m.ac.uk/projects/fastqc/). FASTQs were aligned to the library and processed into counts using the MAGECK-VISPR 'count' function (https://bitbucket.org/liulab/mageck-vispr/src/master/). β-values were calculated using an MLE model generated independently for each comparison. Non-targeting sgRNAs were used to derive a null distribution to determine p-values.

In vitro cytotoxicity and flow cytometry assays

For in vitro cytotoxicity test, CAR T cells were co-cultured with GSCs at an effector: target ratio of 1:40. After 48 hours of co-culture, the numbers of CAR T cells and GSCs were evaluated by flow cytometry. Flow cytometry assays were performed on GSCs, CAR T cells from monoculture or co-culture with procedures described previously (30). For co-culture, anti-CD45 (BD Biosciences Cat# 340665, RRID:AB_400075) staining was used to distinguish GSCs with T cells, and CAR T cells were identified by anti-IL13 (BioLegend Cat# 501914, RRID:AB_2616746) staining. Other antibodies used for flow cytometry target: PD-L1 (Thermo Fisher Scientific Cat# 17–5983-42, RRID:AB_10597586), TIM3 (Thermo Fisher Scientific Cat# 17–3109-42, RRID:AB_1963622), LAG3 (Thermo Fisher Scientific Cat# 12–2239-41, RRID:AB_2572596), PD1 (BioLegend Cat# 329922, RRID:AB_10933429), CD69 (BD Biosciences Cat# 340560, RRID:AB_400523), CD137 (BD Biosciences Cat# 555956, RRID:AB_396252) and IL13Rα2 (BioLegend Cat# 354404, RRID:AB_11218789). All samples were analyzed via a Macsquant Analyzer (Miltenyi Biotec) and processed via FlowJo v10 (RRID:SCR_008520).

RNA-sequencing analysis

Total mRNA from GSCs or CAR T cells was isolated and purified by RNeasy Mini Kit (Qiagen Inc.) and sequenced with Illumina protocols on a HiSeq 2500 to generate 50-bp reads. Trim Galore (https://www.bioinformatics.babraham.ac.uk/projects/trim_galore/) (RRID:SCR_011847) was used to trim adaptors and remove low quality reads. Reads were quantified against Gencode v29 using Salmon (RRID:SCR_017036, https://combine-lab.github.io/salmon/) with correction for fragment-level GC bias, positional bias and sequence-specific bias. Transcripts were summarized to gene level and processed to transcripts per million (TPM) using the R/Bioconductor (https://www.bioconductor.org/) package DESeq2 (RRID:SCR_000154, https://bioconductor.org/packages/release/bio-c/html/DESeq2.html). Comparisons were performed using contrasts in DESeq2 followed by Benjamini-Hochberg adjustment to correct for false discovery rate.

Gene set enrichment analysis

ClueGO gene set enrichment plots were generated using the ClueGO plugin (http://apps.cytoscape.org/apps/cluego, RRID:SCR_005748) for GO BP, KEGG or Reactome gene sets and visualized in Cytoscape v3.7.2 (https://cytoscape.org/). GSEA (RRID:SCR_003199) plots were generated from preranked lists using the mean β value as

the ranking metric. Reactome networks were created using the Reactome FI plugin (https://reactome.org/tools/reactome-fiviz) with network version 2018 and visualized in Cytoscape. Networks were clustered using built-in network clustering algorithm, which utilizes spectral partition-based network clustering, and node layout and color were determined by module assignment. GSEA plots from RNA-sequencing data were generated from preranked lists. Weighting metrics for preranked lists were generated using the DESeq2 results from the gene knockdown vs. non-targeting control and applying the formula: -log10(FDR) * log2(fold change). ssGSEA scores for specific immune or functional pathways were generated using the ssGSEA function from the R/Bioconductor package GSVA (https://bioconductor.org/packages/release/bioc/html/GSVA.html) (94) and plotted using pheatmap (https://cran.r-project.org/web/packages/pheatmap/). ChEA enrichments were performed using Enrichr (https://amp.pharm.mssm.edu/Enrichr/). Barplots for positive or negative gene set enrichments were performed using Metascape (https://metascape.org/gp/index.html) for significantly up- or down-regulated genes (FDR <0.05 and log2 fold change >1 or <−1).

Reactome networks and KEGG pathways

Reactome networks were derived from RNA-seq data using the Cytoscape Reactome FI plugin (RRID:SCR_003032). A gene list of upregulated (FDR <0.05 and log2 fold change >1) or downregulated (FDR <0.05 and log2 fold change <−1) genes plus the target gene (as knockout by CRISPR-Cas9 would not be detected by RNA-seq) was input into Reactome FI and all genes with at least one edge were included in the network plot. Node color (light to dark) and size (small to large) are proportional to node degree. Pathway enrichment was performed on this network of genes using the Reactome FI enrichment option. Boxplots for genes from selected pathways were generated using RNA-seq TPM data. KEGG pathway visualizations were generated using the R/Bioconductor package pathview (https://www.bioconductor.org/packages/release/bioc/html/pathview.html) from for selected pathways and genes were colored based upon the log2 fold change knockout vs. control.

Single cell RNA-sequencing analysis

Single cell RNA-sequencing files were processed using the Cell Ranger workflow (https://support.10xgenomics.com/single-cell-gene-expression/software/overview/welcome). FASTQ files were generated using the Cell Ranger ‘mkfastq’ command with default parameters. FASTQs were aligned to the hg19 genome build using the ‘count’ function and aggregated using the default Cell Ranger ‘aggr’ parameters with normalization performed by subsampling wells to equalize read depth across cells. Downstream analyses were performed using the R/Bioconductor package Seurat (https://satijalab.org/seurat/) (95). Specifically, datasets of stimulated and unstimulated cells in knockout or control populations were merged using the “FindIntegrationAnchors” Seurat function. Clustering was performed using UMAP using PCA for dimensional reduction and a resolution of 0.6 from 1 to 20 dimensions. Dead cell clusters were determined by high expression of mitochondrial genes and removed. Samples were then reclustered. Clusters with similar CD4 or CD8, Ki67 and marker expression, determined using the “FindAllMarkers” function that were proximal on the UMAP projection were merged. All plots for gene expression were generated using normalized data from the default parameters of the “NormalizeData” function. Gene

expression was visualized on the UMAP projection using the “FeaturePlot” function with a maximum cutoff or gene expression determined on a gene-by-gene basis.

Functional analysis of CAR T cells in orthotopic GBM models

All mouse experiments were performed using protocols approved by the City of Hope IACUC. Orthotopic GBM models were generated using 6- to 8 week-old NOD/SCID/IL2R$^{-/-}$ (NSG) mice (IMSR Cat# JAX:005557, RRID:IMSR_JAX:005557), as previously described (96). Briefly, ffLuc-transduced GSCs (1×10^5/mouse) were stereotactically implanted (intracranially) into the right forebrain of NSG mice. Randomization was performed after 8 days of tumor injection based on bioluminescent signal, and mice were then treated intracranially with CAR T cells (2×10^4 or 5×10^4/mouse as indicated for each experiment). To ensure statistical power, all treatment groups include ≥6 animals. Mice were monitored by the Department of Comparative Medicine at City of Hope for survival and any symptoms related to tumor progression, with euthanasia applied according to the American Veterinary Medical Association Guidelines. Studies were done in both male and female animals. Investigators were not blinded for randomization and treatment.

TCGA data analysis

Analysis of genes in the TCGA dataset was performed using RNA-sequencing TCGA GBM data. Immune infiltration signatures were previously reported (97). GSEA plots for each gene in the context of TCGA GBM data were generated by using the normalized gene expression as a continuous phenotype.

CAR T cell responder analysis

Gene sets derived from TLE4 or IKZF2 knockout were analyzed in the context of CAR T cell non-responder vs. responders from a previous report on patients with CLL (27). Genes upregulated in bulk RNA-seq of CAR T cells following knockout of TLE4 or IKZF2 (FDR <0.05 and log2 fold change > 1) were plotted by their fold change expression in stimulated vs. unstimulated CAR T cells for responders or non-responders. Fold change was calculated using DESeq2 for stimulated vs. unstimulated cells independently for each group (non-responder or complete responder). Cluster 10-enriched genes in the TLE4 knockout and control sc-seq data, identified by the “FindAllMarkers” function in Seurat subsetted for overexpressed genes, were plotted similarly. Genes upregulated (>0.4 log2 fold change of normalized counts) in sc-seq for IKZF2 knockout vs. control in stimulated CAR T cells were plotted similarly.

Statistical analysis

CAR T cell functional data (tumor killing, expansion, survival of tumor-bearing mice) were analyzed via GraphPad Prism. Group means ± SEM were plotted. Methods of p-value calculations are indicated in figure legends.

Supplementary Material

Refer to Web version on PubMed Central for supplementary material.

Acknowledgments

We thank our funding sources: NIH: D.W., CA234923; B.C.P., CA217066; R.C.G., CA217065; L.J.Y.K., CA203101; C.E.B., CA236500; J.N.R., CA238662, CA197718, NS203434; Ivy Foundation (C.E.B.); Westlake Education Foundation (Q.X.).

Additional information:

Funding sources: NIH: D.W., CA234923; B.C.P., CA217066; R.C.G., CA217065; L.J.Y.K., CA203101; C.E.B., CA236500; J.N.R., CA238662, CA197718, NS203434; Ivy Foundation (C.E.B.); Westlake Education Foundation (Q.X.). C.E.B. receive royalty payments from Mustang Bio; all other authors declare no competing interests. Patent associated with this study has been submitted (application serial number: 63/117439)

REFERENCES

1. Lim M, Xia Y, Bettegowda C, Weller M. Current state of immunotherapy for glioblastoma. Nat Rev Clin Oncol2018;15(7):422–42 doi 10.1038/s41571-018-0003-5. [PubMed: 29643471]
2. Maude SL, Laetsch TW, Buechner J, Rives S, Boyer M, Bittencourt H, et al.Tisagenlecleucel in Children and Young Adults with B-Cell Lymphoblastic Leukemia. N Engl J Med2018;378(5):439–48 doi 10.1056/NEJMoa1709866. [PubMed: 29385370]
3. Neelapu SS, Locke FL, Bartlett NL, Lekakis LJ, Miklos DB, Jacobson CA, et al.Axicabtagene Ciloleucel CAR T-Cell Therapy in Refractory Large B-Cell Lymphoma. N Engl J Med2017;377(26):2531–44 doi 10.1056/NEJMoa1707447. [PubMed: 29226797]
4. Brown CE, Starr R, Aguilar B, Shami AF, Martinez C, D'Apuzzo M, et al.Stem-like tumor-initiating cells isolated from IL13Ralpha2 expressing gliomas are targeted and killed by IL13-zetakine-redirected T Cells. Clin Cancer Res2012;18(8):2199–209 doi 10.1158/1078-0432.CCR-11-1669. [PubMed: 22407828]
5. Ahmed N, Salsman VS, Kew Y, Shaffer D, Powell S, Zhang YJ, et al.HER2-specific T cells target primary glioblastoma stem cells and induce regression of autologous experimental tumors. Clin Cancer Res2010;16(2):474–85 doi 10.1158/1078-0432.CCR-09-1322. [PubMed: 20068073]
6. Morgan RA, Johnson LA, Davis JL, Zheng Z, Woolard KD, Reap EA, et al.Recognition of glioma stem cells by genetically modified T cells targeting EGFRvIII and development of adoptive cell therapy for glioma. Hum Gene Ther2012;23(10):1043–53 doi 10.1089/hum.2012.041. [PubMed: 22780919]
7. Brown CE, Badie B, Barish ME, Weng L, Ostberg JR, Chang WC, et al.Bioactivity and Safety of IL13Ralpha2-Redirected Chimeric Antigen Receptor CD8+ T Cells in Patients with Recurrent Glioblastoma. Clin Cancer Res2015;21(18):4062–72 doi 10.1158/1078-0432.CCR-15-0428. [PubMed: 26059190]
8. Brown CE, Alizadeh D, Starr R, Weng L, Wagner JR, Naranjo A, et al.Regression of Glioblastoma after Chimeric Antigen Receptor T-Cell Therapy. The New England journal of medicine2016;375(26):2561–9 doi 10.1056/NEJMoa1610497. [PubMed: 28029927]
9. Ahmed N, Brawley V, Hegde M, Bielamowicz K, Kalra M, Landi D, et al.HER2-Specific Chimeric Antigen Receptor-Modified Virus-Specific T Cells for Progressive Glioblastoma: A Phase 1 Dose-Escalation Trial. JAMA Oncol2017;3(8):1094–101 doi 10.1001/jamaoncol.2017.0184. [PubMed: 28426845]
10. O'Rourke DM, Nasrallah MP, Desai A, Melenhorst JJ, Mansfield K, Morrissette JJD, et al.A single dose of peripherally infused EGFRvIII-directed CAR T cells mediates antigen loss and induces adaptive resistance in patients with recurrent glioblastoma. Sci Transl Med2017;9(399) doi 10.1126/scitranslmed.aaa0984.
11. Akhavan D, Alizadeh D, Wang D, Weist MR, Shepphird JK, Brown CE. CAR T cells for brain tumors: Lessons learned and road ahead. Immunological reviews2019;290(1):60–84 doi 10.1111/imr.12773. [PubMed: 31355493]
12. Chuntova P, Downey KM, Hegde B, Almeida ND, Okada H. Genetically Engineered T-Cells for Malignant Glioma: Overcoming the Barriers to Effective Immunotherapy. Front Immunol2018;9:3062 doi 10.3389/fimmu.2018.03062. [PubMed: 30740109]

13. Lim WA, June CH. The Principles of Engineering Immune Cells to Treat Cancer. Cell2017;168(4):724–40 doi 10.1016/j.cell.2017.01.016. [PubMed: 28187291]
14. Simeonov DR, Marson A. CRISPR-Based Tools in Immunity. Annual review of immunology2019;37:571–97 doi 10.1146/annurev-immunol-042718-041522.
15. Stadtmauer EA, Fraietta JA, Davis MM, Cohen AD, Weber KL, Lancaster E, et al.CRISPR-engineered T cells in patients with refractory cancer. Science (New York, NY)2020;367(6481) doi 10.1126/science.aba7365.
16. Tang N, Cheng C, Zhang X, Qiao M, Li N, Mu W, et al.TGF-beta inhibition via CRISPR promotes the long-term efficacy of CAR T cells against solid tumors. JCI Insight2020;5(4) doi 10.1172/jci.insight.133977.
17. Crowther MD, Dolton G, Legut M, Caillaud ME, Lloyd A, Attaf M, et al.Genome-wide CRISPR-Cas9 screening reveals ubiquitous T cell cancer targeting via the monomorphic MHC class I-related protein MR1. Nature immunology2020;21(2):178–85 doi 10.1038/s41590-019-0578-8. [PubMed: 31959982]
18. Manguso RT, Pope HW, Zimmer MD, Brown FD, Yates KB, Miller BC, et al.In vivo CRISPR screening identifies Ptpn2 as a cancer immunotherapy target. Nature2017;547(7664):413–8 doi 10.1038/nature23270. [PubMed: 28723893]
19. Patel SJ, Sanjana NE, Kishton RJ, Eidizadeh A, Vodnala SK, Cam M, et al.Identification of essential genes for cancer immunotherapy. Nature2017;548(7669):537–42 doi 10.1038/nature23477. [PubMed: 28783722]
20. Dong MB, Wang G, Chow RD, Ye L, Zhu L, Dai X, et al.Systematic Immunotherapy Target Discovery Using Genome-Scale In Vivo CRISPR Screens in CD8 T Cells. Cell2019;178(5):1189–204e23 doi 10.1016/j.cell.2019.07.044. [PubMed: 31442407]
21. Shifrut E, Carnevale J, Tobin V, Roth TL, Woo JM, Bui CT, et al.Genome-wide CRISPR Screens in Primary Human T Cells Reveal Key Regulators of Immune Function. Cell2018;175(7):1958–71e15 doi 10.1016/j.cell.2018.10.024. [PubMed: 30449619]
22. Wei J, Long L, Zheng W, Dhungana Y, Lim SA, Guy C, et al.Targeting REGNASE-1 programs long-lived effector T cells for cancer therapy. Nature2019;576(7787):471–6 doi 10.1038/s41586-019-1821-z. [PubMed: 31827283]
23. Harris DT, Hager MV, Smith SN, Cai Q, Stone JD, Kruger P, et al.Comparison of T Cell Activities Mediated by Human TCRs and CARs That Use the Same Recognition Domains. J Immunol2018;200(3):1088–100 doi 10.4049/jimmunol.1700236. [PubMed: 29288199]
24. Lathia JD, Mack SC, Mulkearns-Hubert EE, Valentim CL, Rich JN. Cancer stem cells in glioblastoma. Genes & development2015;29(12):1203–17 doi 10.1101/gad.261982.115. [PubMed: 26109046]
25. Prager BC, Xie Q, Bao S, Rich JN. Cancer Stem Cells: The Architects of the Tumor Ecosystem. Cell Stem Cell2019;24(1):41–53 doi 10.1016/j.stem.2018.12.009. [PubMed: 30609398]
26. Brown CE, Aguilar B, Starr R, Yang X, Chang WC, Weng L, et al.Optimization of IL13Ralpha2-Targeted Chimeric Antigen Receptor T Cells for Improved Anti-tumor Efficacy against Glioblastoma. Molecular therapy : the journal of the American Society of Gene Therapy2018;26(1):31–44 doi 10.1016/j.ymthe.2017.10.002. [PubMed: 29103912]
27. Fraietta JA, Lacey SF, Orlando EJ, Pruteanu-Malinici I, Gohil M, Lundh S, et al.Determinants of response and resistance to CD19 chimeric antigen receptor (CAR) T cell therapy of chronic lymphocytic leukemia. Nat Med2018;24(5):563–71 doi 10.1038/s41591-018-0010-1. [PubMed: 29713085]
28. Rossi J, Paczkowski P, Shen YW, Morse K, Flynn B, Kaiser A, et al.Preinfusion polyfunctional anti-CD19 chimeric antigen receptor T cells are associated with clinical outcomes in NHL. Blood2018;132(8):804–14 doi 10.1182/blood-2018-01-828343. [PubMed: 29895668]
29. Singh N, Lee YG, Shestova O, Ravikumar P, Hayer KE, Hong SJ, et al.Impaired Death Receptor Signaling in Leukemia Causes Antigen-Independent Resistance by Inducing CAR T-cell Dysfunction. Cancer discovery2020;10(4):552–67 doi 10.1158/2159-8290.CD-19-0813. [PubMed: 32001516]

30. Wang D, Aguilar B, Starr R, Alizadeh D, Brito A, Sarkissian A, et al.Glioblastoma-targeted CD4+ CAR T cells mediate superior antitumor activity. JCI insight2018;3(10):e99048 doi 10.1172/jci.insight.99048.

31. Wang D, Starr R, Alizadeh D, Yang X, Forman SJ, Brown CE. In Vitro Tumor Cell Rechallenge For Predictive Evaluation of Chimeric Antigen Receptor T Cell Antitumor Function. Journal of visualized experiments : JoVE2019(144) doi 10.3791/59275.

32. Doench JG, Fusi N, Sullender M, Hegde M, Vaimberg EW, Donovan KF, et al.Optimized sgRNA design to maximize activity and minimize off-target effects of CRISPR-Cas9. Nature biotechnology2016;34(2):184–91 doi 10.1038/nbt.3437.

33. Brown CE, Warden CD, Starr R, Deng X, Badie B, Yuan YC, et al.Glioma IL13Ralpha2 is associated with mesenchymal signature gene expression and poor patient prognosis. PLoS One2013;8(10):e77769 doi 10.1371/journal.pone.0077769. [PubMed: 24204956]

34. Silva-Filho JL, Caruso-Neves C, Pinheiro AAS. IL-4: an important cytokine in determining the fate of T cells. Biophys Rev2014;6(1):111–8 doi 10.1007/s12551-013-0133-z. [PubMed: 28509961]

35. Crawford A, Angelosanto JM, Kao C, Doering TA, Odorizzi PM, Barnett BE, et al.Molecular and transcriptional basis of CD4(+) T cell dysfunction during chronic infection. Immunity2014;40(2):289–302 doi 10.1016/j.immuni.2014.01.005. [PubMed: 24530057]

36. Martinez GJ, Pereira RM, Aijo T, Kim EY, Marangoni F, Pipkin ME, et al.The transcription factor NFAT promotes exhaustion of activated CD8(+) T cells. Immunity2015;42(2):265–78 doi 10.1016/j.immuni.2015.01.006. [PubMed: 25680272]

37. Khan O, Giles JR, McDonald S, Manne S, Ngiow SF, Patel KP, et al.TOX transcriptionally and epigenetically programs CD8(+) T cell exhaustion. Nature2019;571(7764):211–8 doi 10.1038/s41586-019-1325-x. [PubMed: 31207603]

38. Dong Y, Li X, Yu Y, Lv F, Chen Y. JAK/STAT signaling is involved in IL-35-induced inhibition of hepatitis B virus antigen-specific cytotoxic T cell exhaustion in chronic hepatitis B. Life Sci2020;252:117663 doi 10.1016/j.lfs.2020.117663. [PubMed: 32302624]

39. Ma X, Bi E, Lu Y, Su P, Huang C, Liu L, et al.Cholesterol Induces CD8(+) T Cell Exhaustion in the Tumor Microenvironment. Cell metabolism2019;30(1):143–56e5 doi 10.1016/j.cmet.2019.04.002. [PubMed: 31031094]

40. Chen J, Lopez-Moyado IF, Seo H, Lio CJ, Hempleman LJ, Sekiya T, et al.NR4A transcription factors limit CAR T cell function in solid tumours. Nature2019;567(7749):530–4 doi 10.1038/s41586-019-0985-x. [PubMed: 30814732]

41. Singh U, Shamran H, Singh N, Guan HB, Mishra M, Price RL, et al.Blocking fatty acid amide hydrolase reduces T cell activation and attenuates experimental colitis. Journal of Immunology2015;194.

42. Schmitz ML, Krappmann D. Controlling NF-kappa B activation in T cells by costimulatory receptors. Cell Death and Differentiation2006;13(5):834–42 doi 10.1038/sj.cdd.4401845. [PubMed: 16410801]

43. Eyquem J, Mansilla-Soto J, Giavridis T, van der Stegen SJ, Hamieh M, Cunanan KM, et al.Targeting a CAR to the TRAC locus with CRISPR/Cas9 enhances tumour rejection. Nature2017;543(7643):113–7 doi 10.1038/nature21405. [PubMed: 28225754]

44. Wang D, Starr R, Chang WC, Aguilar B, Alizadeh D, Wright SL, et al.Chlorotoxin-directed CAR T cells for specific and effective targeting of glioblastoma. Sci Transl Med2020;12(533) doi 10.1126/scitranslmed.aaw2672.

45. Bandyopadhyay S, Valdor R, Macian F. Tle4 regulates epigenetic silencing of gamma interferon expression during effector T helper cell tolerance. Molecular and cellular biology2014;34(2):233–45 doi 10.1128/MCB.00902-13. [PubMed: 24190972]

46. Naluyima P, Lal KG, Costanzo MC, Kijak GH, Gonzalez VD, Blom K, et al.Terminal Effector CD8 T Cells Defined by an IKZF2(+)IL-7R(−) Transcriptional Signature Express FcgammaRIIIA, Expand in HIV Infection, and Mediate Potent HIV-Specific Antibody-Dependent Cellular Cytotoxicity. J Immunol2019;203(8):2210–21 doi 10.4049/jimmunol.1900422. [PubMed: 31519862]

47. Sowell RT, Kaech SM. Probing the Diversity of T Cell Dysfunction in Cancer. Cell2016;166(6):1362–4 doi 10.1016/j.cell.2016.08.058. [PubMed: 27610560]

48. Shin HJ, Lee JB, Park SH, Chang J, Lee CW. T-bet expression is regulated by EGR1-mediated signaling in activated T cells. Clin Immunol2009;131(3):385–94 doi 10.1016/j.clim.2009.02.009. [PubMed: 19307156]
49. Ananieva EA, Patel CH, Drake CH, Powell JD, Hutson SM. Cytosolic branched chain aminotransferase (BCATc) regulates mTORC1 signaling and glycolytic metabolism in CD4+ T cells. The Journal of biological chemistry2014;289(27):18793–804 doi 10.1074/jbc.M114.554113. [PubMed: 24847056]
50. Hess C, Means TK, Autissier P, Woodberry T, Altfeld M, Addo MM, et al.IL-8 responsiveness defines a subset of CD8 T cells poised to kill. Blood2004;104(12):3463–71 doi 10.1182/blood-2004-03-1067. [PubMed: 15292066]
51. Trifilo MJ, Bergmann CC, Kuziel WA, Lane TE. CC chemokine ligand 3 (CCL3) regulates CD8(+)-T-cell effector function and migration following viral infection. Journal of virology2003;77(7):4004–14 doi 10.1128/jvi.77.7.4004-4014.2003. [PubMed: 12634360]
52. Kiniry BE, Hunt PW, Hecht FM, Somsouk M, Deeks SG, Shacklett BL. Differential Expression of CD8(+) T Cell Cytotoxic Effector Molecules in Blood and Gastrointestinal Mucosa in HIV-1Infection. J Immunol2018;200(5):1876–88 doi 10.4049/jimmunol.1701532. [PubMed: 29352005]
53. Duraiswamy J, Ibegbu CC, Masopust D, Miller JD, Araki K, Doho GH, et al.Phenotype, function, and gene expression profiles of programmed death-1(hi) CD8 T cells in healthy human adults. J Immunol2011;186(7):4200–12 doi 10.4049/jimmunol.1001783. [PubMed: 21383243]
54. Wherry EJ, Ha SJ, Kaech SM, Haining WN, Sarkar S, Kalia V, et al.Molecular signature of CD8+ T cell exhaustion during chronic viral infection. Immunity2007;27(4):670–84 doi 10.1016/j.immuni.2007.09.006. [PubMed: 17950003]
55. Lynn RC, Weber EW, Sotillo E, Gennert D, Xu P, Good Z, et al.c-Jun overexpression in CAR T cells induces exhaustion resistance. Nature2019;576(7786):293–300 doi 10.1038/s41586-019-1805-z. [PubMed: 31802004]
56. Muller MR, Rao A. NFAT, immunity and cancer: a transcription factor comes of age. Nat Rev Immunol2010;10(9):645–56 doi 10.1038/nri2818. [PubMed: 20725108]
57. Myers LM, Tal MC, Torrez Dulgeroff LB, Carmody AB, Messer RJ, Gulati G, et al.A functional subset of CD8(+) T cells during chronic exhaustion is defined by SIRPalpha expression. Nature communications2019;10(1):794 doi 10.1038/s41467-019-08637-9.
58. Maimela NR, Liu S, Zhang Y. Fates of CD8+ T cells in Tumor Microenvironment. Comput Struct Biotechnol J2019;17:1–13 doi 10.1016/j.csbj.2018.11.004. [PubMed: 30581539]
59. Bhairavabhotla R, Kim YC, Glass DD, Escobar TM, Patel MC, Zahr R, et al.Transcriptome profiling of human FoxP3+ regulatory T cells. Hum Immunol2016;77(2):201–13 doi 10.1016/j.humimm.2015.12.004. [PubMed: 26686412]
60. Nishio H, Yaguchi T, Sugiyama J, Sumimoto H, Umezawa K, Iwata T, et al.Immunosuppression through constitutively activated NF-kappa B signalling in human ovarian cancer and its reversal by an NF-kappa B inhibitor. British Journal of Cancer2014;110(12):2965–74 doi 10.1038/bjc.2014.251. [PubMed: 24867687]
61. Yamamoto Y, Gaynor RB. Therapeutic potential of inhibition of the NF-kappaB pathway in the treatment of inflammation and cancer. The Journal of clinical investigation2001;107(2):135–42 doi 10.1172/JCI11914. [PubMed: 11160126]
62. Liao W, Overman MJ, Boutin AT, Shang X, Zhao D, Dey P, et al.KRAS-IRF2 Axis Drives Immune Suppression and Immune Therapy Resistance in Colorectal Cancer. Cancer Cell2019;35(4):559–72e7 doi 10.1016/j.ccell.2019.02.008. [PubMed: 30905761]
63. Li WM, Liu HR. CCL20-CCR6 Cytokine Network Facilitate Treg Activity in Advanced Grades and Metastatic Variants of Hepatocellular Carcinoma. Scand J Immunol2016;83(1):33–7 doi 10.1111/sji.12367. [PubMed: 26331965]
64. Do Y, Nagarkatti PS, Nagarkatti M. Role of CD44 and hyaluronic acid (HA) in activation of alloreactive and antigen-specific T cells by bone marrow-derived dendritic cells. Journal of immunotherapy (Hagerstown, Md : 1997)2004;27(1):1–12 doi 10.1097/00002371-200401000-00001.

65. Jankowska KI, Williamson EK, Roy NH, Blumenthal D, Chandra V, Baumgart T, et al.Integrins Modulate T Cell Receptor Signaling by Constraining Actin Flow at the Immunological Synapse. Frontiers in Immunology2018;9 doi ARTN 2510.3389/fimmu.2018.00025.
66. Brown CE, Alizadeh D, Starr R, Weng L, Wagner JR, Naranjo A, et al.Regression of Glioblastoma after Chimeric Antigen Receptor T-Cell Therapy. N Engl J Med2016;375(26):2561–9 doi 10.1056/NEJMoa1610497. [PubMed: 28029927]
67. Batlle E, Massague J. Transforming Growth Factor-beta Signaling in Immunity and Cancer. Immunity2019;50(4):924–40 doi 10.1016/j.immuni.2019.03.024. [PubMed: 30995507]
68. Deng Q, Han G, Puebla-Osorio N, Ma MCJ, Strati P, Chasen B, et al.Characteristics of anti-CD19 CAR T cell infusion products associated with efficacy and toxicity in patients with large B cell lymphomas. Nat Med2020 doi 10.1038/s41591-020-1061-7.
69. Ghassemi S, Nunez-Cruz S, O'Connor RS, Fraietta JA, Patel PR, Scholler J, et al.Reducing Ex Vivo Culture Improves the Antileukemic Activity of Chimeric Antigen Receptor (CAR) T Cells. Cancer Immunol Res2018;6(9):1100–9 doi 10.1158/2326-6066.CIR-17-0405. [PubMed: 30030295]
70. Mount CW, Majzner RG, Sundaresh S, Arnold EP, Kadapakkam M, Haile S, et al.Potent antitumor efficacy of anti-GD2 CAR T cells in H3-K27M+ diffuse midline gliomas. Nature Medicine2018;24(5):572–9 doi 10.1038/s41591-018-0006-x.
71. Theruvath J, Sotillo E, Mount CW, Graef CM, Delaidelli A, Heitzeneder S, et al.Locoregionally administered B7-H3-targeted CAR T cells for treatment of atypical teratoid/rhabdoid tumors. Nat Med2020;26(5):712–9 doi 10.1038/s41591-020-0821-8. [PubMed: 32341579]
72. Donovan LK, Delaidelli A, Joseph SK, Bielamowicz K, Fousek K, Holgado BL, et al.Locoregional delivery of CAR T cells to the cerebrospinal fluid for treatment of metastatic medulloblastoma and ependymoma. Nat Med2020;26(5):720–31 doi 10.1038/s41591-020-0827-2. [PubMed: 32341580]
73. Ye L, Park JJ, Dong MB, Yang Q, Chow RD, Peng L, et al.In vivo CRISPR screening in CD8 T cells with AAV-Sleeping Beauty hybrid vectors identifies membrane targets for improving immunotherapy for glioblastoma. Nature biotechnology2019;37(11):1302–13 doi 10.1038/s41587-019-0246-4.
74. Arvanitis CD, Ferraro GB, Jain RK. The blood-brain barrier and blood-tumour barrier in brain tumours and metastases. Nat Rev Cancer2020;20(1):26–41 doi 10.1038/s41568-019-0205-x. [PubMed: 31601988]
75. Platt RJ, Chen S, Zhou Y, Yim MJ, Swiech L, Kempton HR, et al.CRISPR-Cas9 knockin mice for genome editing and cancer modeling. Cell2014;159(2):440–55 doi 10.1016/j.cell.2014.09.014. [PubMed: 25263330]
76. Henriksson J, Chen X, Gomes T, Ullah U, Meyer KB, Miragaia R, et al.Genome-wide CRISPR Screens in T Helper Cells Reveal Pervasive Crosstalk between Activation and Differentiation. Cell2019;176(4):882–96e18 doi 10.1016/j.cell.2018.11.044. [PubMed: 30639098]
77. Brown CE, Mackall CL. CAR T cell therapy: inroads to response and resistance. Nat Rev Immunol2019;19(2):73–4 doi 10.1038/s41577-018-0119-y. [PubMed: 30631206]
78. Wherry EJ, Kurachi M. Molecular and cellular insights into T cell exhaustion. Nat Rev Immunol2015;15(8):486–99 doi 10.1038/nri3862. [PubMed: 26205583]
79. Long AH, Haso WM, Shern JF, Wanhainen KM, Murgai M, Ingaramo M, et al.4–1BB costimulation ameliorates T cell exhaustion induced by tonic signaling of chimeric antigen receptors. Nat Med2015;21(6):581–90 doi 10.1038/nm.3838. [PubMed: 25939063]
80. Cherkassky L, Morello A, Villena-Vargas J, Feng Y, Dimitrov DS, Jones DR, et al.Human CAR T cells with cell-intrinsic PD-1 checkpoint blockade resist tumor-mediated inhibition. The Journal of clinical investigation2016;126(8):3130–44 doi 10.1172/JCI83092. [PubMed: 27454297]
81. Rafiq S, Yeku OO, Jackson HJ, Purdon TJ, van Leeuwen DG, Drakes DJ, et al.Targeted delivery of a PD-1-blocking scFv by CAR-T cells enhances anti-tumor efficacy in vivo. Nature biotechnology2018;36(9):847–56 doi 10.1038/nbt.4195.
82. Schietinger A, Philip M, Krisnawan VE, Chiu EY, Delrow JJ, Basom RS, et al.Tumor-Specific T Cell Dysfunction Is a Dynamic Antigen-Driven Differentiation Program Initiated Early during Tumorigenesis. Immunity2016;45(2):389–401 doi 10.1016/j.immuni.2016.07.011. [PubMed: 27521269]

83. Man K, Gabriel SS, Liao Y, Gloury R, Preston S, Henstridge DC, et al.Transcription Factor IRF4 Promotes CD8(+) T Cell Exhaustion and Limits the Development of Memory-like T Cells during Chronic Infection. Immunity2017;47(6):1129–41e5 doi 10.1016/j.immuni.2017.11.021. [PubMed: 29246443]
84. Li P, Spolski R, Liao W, Wang L, Murphy TL, Murphy KM, et al.BATF-JUN is critical for IRF4-mediated transcription in T cells. Nature2012;490(7421):543–6 doi 10.1038/nature11530. [PubMed: 22992523]
85. Meixner A, Karreth F, Kenner L, Wagner EF. JunD regulates lymphocyte proliferation and T helper cell cytokine expression. The EMBO journal2004;23(6):1325–35 doi 10.1038/sj.emboj.7600133. [PubMed: 15029240]
86. Chiu R, Angel P, Karin M. Jun-B differs in its biological properties from, and is a negative regulator of, c-Jun. Cell1989;59(6):979–86 doi 10.1016/0092-8674(89)90754-x. [PubMed: 2513128]
87. Wei F, Zhong S, Ma Z, Kong H, Medvec A, Ahmed R, et al.Strength of PD-1 signaling differentially affects T-cell effector functions. Proc Natl Acad Sci U S A2013;110(27):E2480–9 doi 10.1073/pnas.1305394110. [PubMed: 23610399]
88. Jiao S, Subudhi SK, Aparicio A, Ge Z, Guan B, Miura Y, et al.Differences in Tumor Microenvironment Dictate T Helper Lineage Polarization and Response to Immune Checkpoint Therapy. Cell2019;179(5):1177–90e13 doi 10.1016/j.cell.2019.10.029. [PubMed: 31730856]
89. Tran E, Turcotte S, Gros A, Robbins PF, Lu YC, Dudley ME, et al.Cancer immunotherapy based on mutation-specific CD4+ T cells in a patient with epithelial cancer. Science (New York, NY)2014;344(6184):641–5 doi 10.1126/science.1251102.
90. Lee DW, Kochenderfer JN, Stetler-Stevenson M, Cui YK, Delbrook C, Feldman SA, et al.T cells expressing CD19 chimeric antigen receptors for acute lymphoblastic leukaemia in children and young adults: a phase 1 dose-escalation trial. Lancet2015;385(9967):517–28 doi 10.1016/S0140-6736(14)61403-3. [PubMed: 25319501]
91. Bao S, Wu Q, McLendon RE, Hao Y, Shi Q, Hjelmeland AB, et al.Glioma stem cells promote radioresistance by preferential activation of the DNA damage response. Nature2006;444(7120):756–60 doi 10.1038/nature05236. [PubMed: 17051156]
92. Xie Q, Wu TP, Gimple RC, Li Z, Prager BC, Wu Q, et al. N(6)-methyladenine DNA Modification in Glioblastoma. Cell 2018;175(5):1228–43 e20 doi 10.1016/j.cell.2018.10.006. [PubMed: 30392959]
93. Priceman SJ, Tilakawardane D, Jeang B, Aguilar B, Murad JP, Park AK, et al.Regional Delivery of Chimeric Antigen Receptor-Engineered T Cells Effectively Targets HER2(+) Breast Cancer Metastasis to the Brain. Clin Cancer Res2018;24(1):95–105 doi 10.1158/1078-0432.ccr-17-2041. [PubMed: 29061641]
94. Hanzelmann S, Castelo R, Guinney J. GSVA: gene set variation analysis for microarray and RNA-seq data. BMC Bioinformatics2013;14:7 doi 10.1186/1471-2105-14-7. [PubMed: 23323831]
95. Stuart T, Butler A, Hoffman P, Hafemeister C, Papalexi E, Mauck WM, 3rd, et al.Comprehensive Integration of Single-Cell Data. Cell2019;177(7):1888–902e21 doi 10.1016/j.cell.2019.05.031. [PubMed: 31178118]
96. Brown CE, Starr R, Martinez C, Aguilar B, D'Apuzzo M, Todorov I, et al.Recognition and killing of brain tumor stem-like initiating cells by CD8+ cytolytic T cells. Cancer Res2009;69(23):8886–93 doi 10.1158/0008-5472.CAN-09-2687. [PubMed: 19903840]
97. Thorsson V, Gibbs DL, Brown SD, Wolf D, Bortone DS, Ou Yang TH, et al.The Immune Landscape of Cancer. Immunity2018;48(4):812–30e14 doi 10.1016/j.immuni.2018.03.023. [PubMed: 29628290]

SIGNIFICANCE

Reciprocal CRISPR screening identified genes in both CAR T cells and tumor cells regulating the potency of CAR T cell cytotoxicity, informing molecular targeting strategies to potentiate CAR T cell antitumor efficacy and elucidate genetic modifications of tumor cells in combination with CAR T cells to advance immuno-oncotherapy.

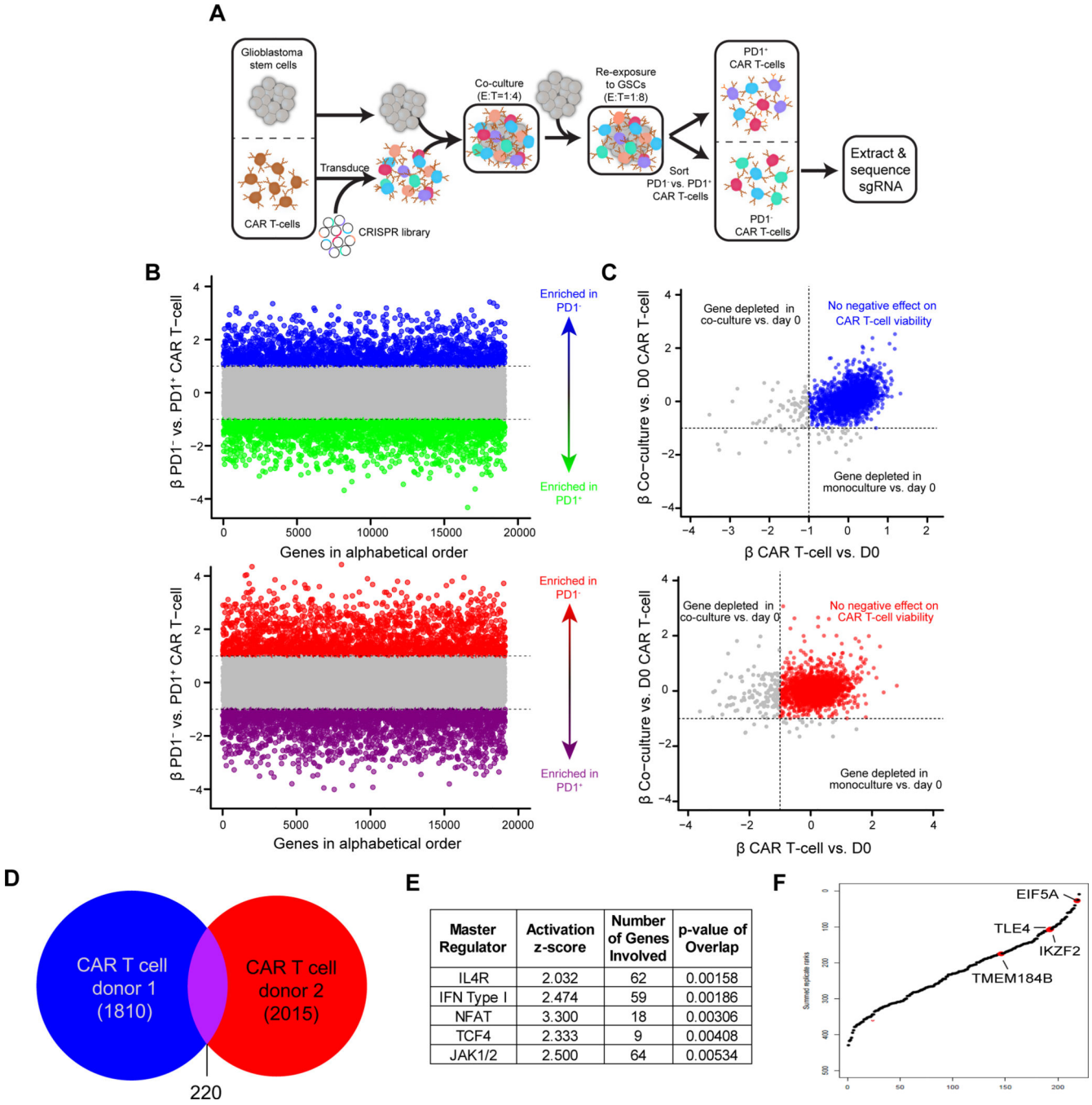

Master Regulator	Activation z-score	Number of Genes Involved	p-value of Overlap
IL4R	2.032	62	0.00158
IFN Type I	2.474	59	0.00186
NFAT	3.300	18	0.00306
TCF4	2.333	9	0.00408
JAK1/2	2.500	64	0.00534

Figure 1. CRISPR-Cas9 screen in CAR T cells co-cultured with GSCs.

A, Overview of screen design. CAR T-cells were transduced with a whole-genome CRISPR-Cas9 library and co-cultured with GSCs, followed by a GSC rechallenge after 48 hours. At the conclusion of the screen (24 hours after the rechallenge), CAR T-cells were sorted for PD1 positivity and $PD1^+$ or $PD1^-$ CAR T-cells were sequenced separately to identify enriched and depleted guides. **B,** Screen results in two replicates of independent donors with genes ordered alphabetically on the x-axis. The MAGECK β-value for each gene comparing $PD1^-$ vs. $PD1^+$ is plotted on the y-axis. Genes enriched in $PD1^-$ cells at a β-value >1 are

in blue or red and genes with a β-value of <−1 (enriched in $PD1^+$ cells) are in green or purple. **C,** Plot of hits from (b) to exclude genes that are depleted following co-culture of CAR T-cells with GSCs (β-value <−1 on the y-axis) or in monoculture (β-value <−1 on the x-axis). Genes in blue or red are not depleted in either condition. **D,** Venn diagram illustrating common hits for depleted genes in two distinct T cell donors. **E,** Ingenuity Pathway Analysis of master regulators (top 5 based on p-values) of 220 overlapping genes in two T cell donors. **F,** Common hits ranked by β-value in a combined model for $PD1^-$ vs. $PD1^+$ CAR T-cells. Labeled hits were selected for validation.

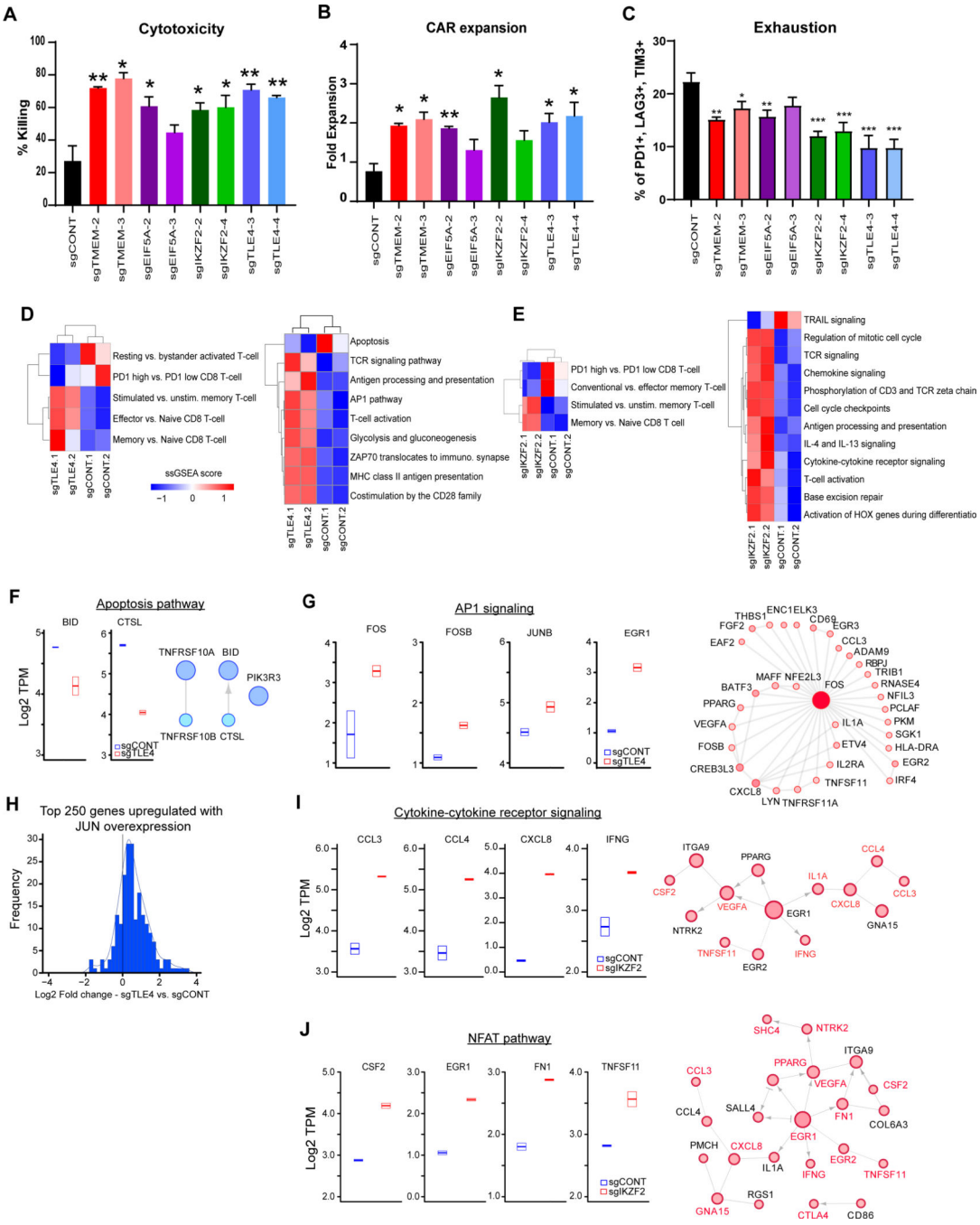

Figure 2. Targets on CAR T cells improves effector potency and alter transcriptional profiles.

A, Killing of CAR T cells with TLE4-, IKZF2-, TMEM184B- or EIF5A-KO against co-cultured GSCs (E:T=1:40, 48 hours). **B,** Expansion of CAR T cells with different knockouts in co-culture with GSCs (E:T=1:40, 48 hours). **C**, CAR T cells with targeted KOs of specific genes were co-cultured with PBT030–2 cells (E:T=1:4) for 48 hours, and re-challenged with tumor cells against (E:T=1:8) for 24 hours, and then analyzed for the expression of exhaustion markers. (A,B,C) *p<0.05, **p<0.01, ***p<0.001 compared to CAR T cells transduced with non-targeting sgRNA (black) using unpaired Student's t tests. **D** and **E,**

Unsupervised clustering of ssGSEA scores comparing TLE4-KO (C) or IKZF2-KO (D) vs. sgCONT CAR T cells for the signatures of selected T cell populations (left) or immune and functional pathways (right). **F,** Left: Boxplot of genes involved in apoptotic signaling from RNA-sequencing data in sgCONT (blue) vs. sgTLE4 (red). Right: Reactome network of genes downregulated following TLE4 knockout that are involved in apoptotic signaling. **G,** Left: Boxplot of genes involved in AP1 signaling from RNA-sequencing data in control (blue) vs. TLE4KO (red) cells. Right: Reactome network of genes upregulated with TLE4 knockout that are linked to FOS. Increasing node size and fill hue are proportional to node degree. **H,** Histogram of log2 fold change of gene expression (comparing TLE4KO vs. control) for 250 genes previously shown to be upregulated with JUN overexpression. **I,** Left: Boxplot of genes involved in cytokine receptor signaling from RNA-sequencing data in control (blue) vs. IKZF2KO (red) cells. Right: Reactome network of genes upregulated with IKZF2-KO that are linked to a gene in the cytokine receptor signaling pathway (labeled in red). Increasing node size and fill hue are proportional to node degree. **J,** Left: Boxplot of genes in the NFAT pathways from RNA-sequencing data in control (blue) vs. IKZF2KO (red) cells. Right: Reactome network of genes upregulated with IKZF2-KO that are linked to upregulated genes in the NFAT pathway (labeled in red).

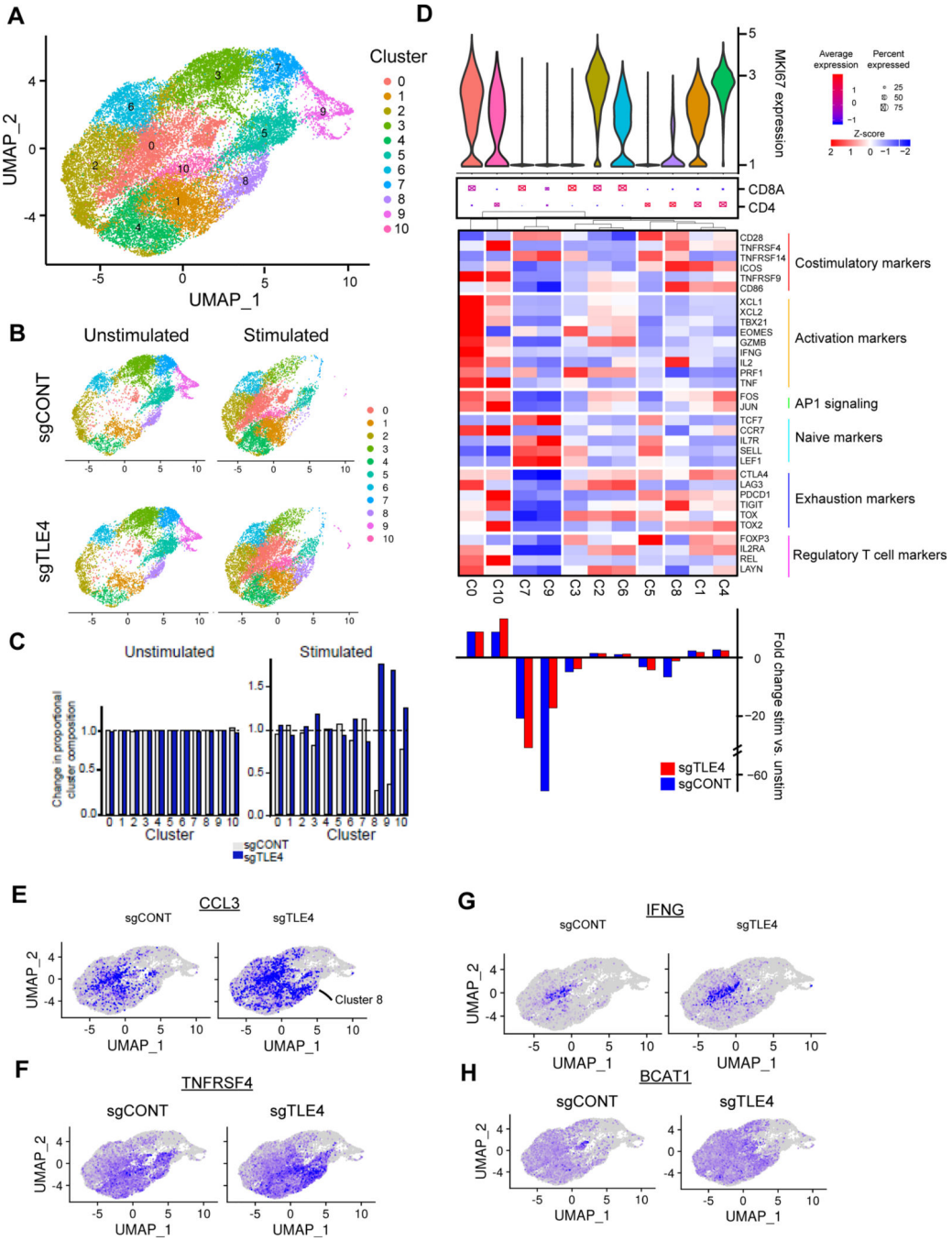

Figure 3. The effect of TLE4KO on CAR T cell subpopulations.

A, UMAP projection of single cell RNA sequencing of control and TLE4KO CAR T cells both before and after stimulation with GSCs. Cluster assignments for the overall population are shown. **B,** Cluster composition of unstimulated vs. unstimulated control or TLE4KO cell populations. **C,** Population distribution of control and TLE4KO CAR T cells before and after stimulation. **D,** Characterization of clusters based upon cell proliferation. Top: Violin plot of MKI67 expression. Middle: Dot plot of CD4 vs. CD8A expression wherein larger dots indicate a higher proportion of cells with expression and red vs. blue

fill indicates higher expression. Heatmap: Scaled expression of T cell markers including costimulatory, activation, naive, exhaustion and regulatory T cell markers as well as AP1 signaling. Bottom: Proportion of cells in each cluster under stimulated vs. unstimulated conditions in control (blue) or TLE4KO (red) populations. Positive values indicate increase in cluster occupancy following stimulation. **E-H,** Expression of CCL3 (E), TNFRSF4 (F), IFNG (G) and BCAT1 (H) in control or TLE4KO CAR T-cells superimposed on the UMAP projection.

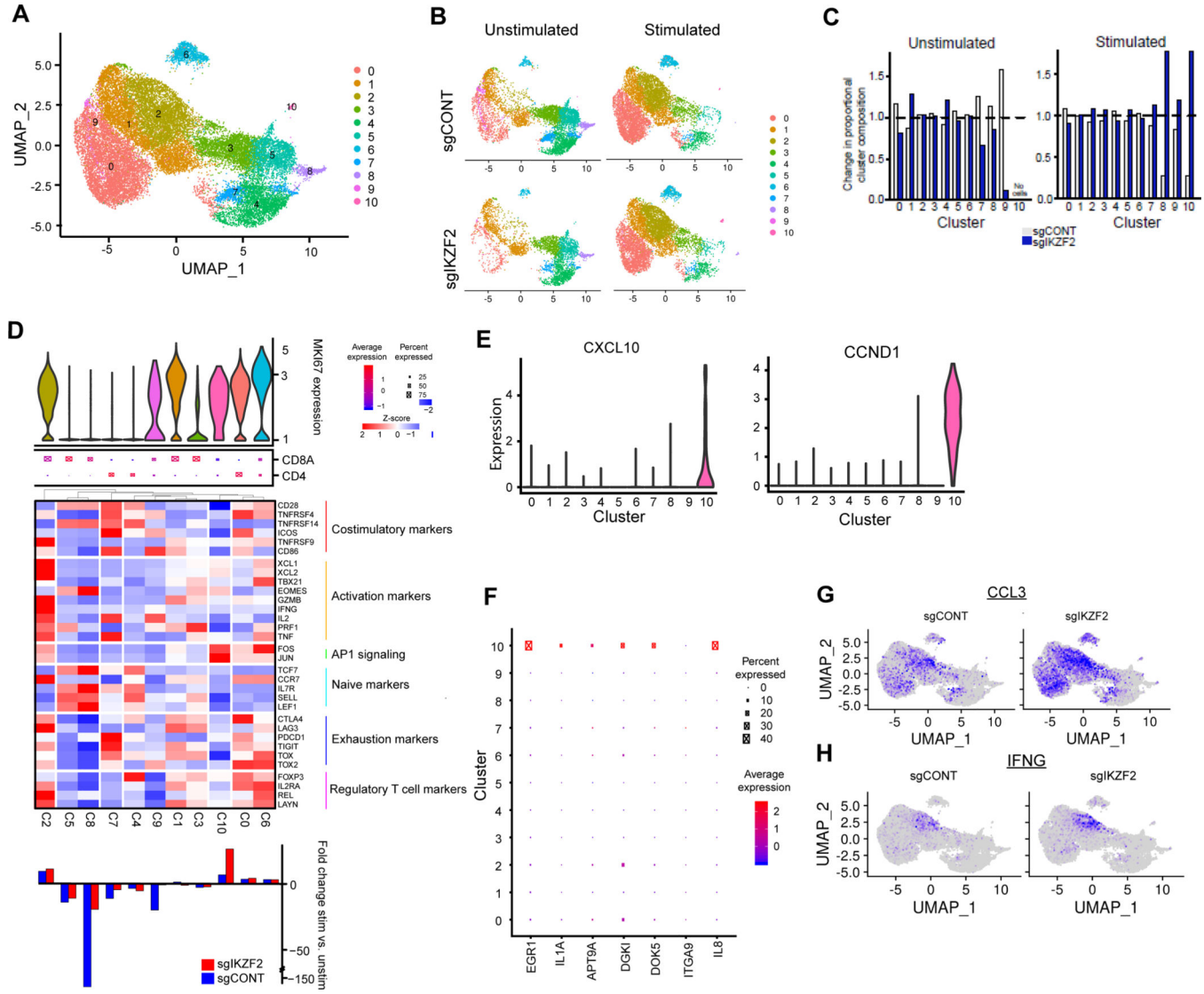

Figure 4. IKZF2 regulates CAR T cell subpopulations.

A, UMAP projection of single cell RNA sequencing of control and IKZF2KO CAR T-cells both before and after stimulation with GSCs. Top: Cluster assignments for the overall population. **B,** Cluster composition of unstimulated vs. unstimulated control or IKZF2KO cell populations. **C,** Population distribution of control and IKZF2KO CAR T cells before and after stimulation. **D,** Characterization of clusters based upon cell proliferation. Top: Violin plot of MKI67 expression. Middle: Dot plot of CD4 vs. CD8A expression wherein larger dots indicate a higher proportion of cells with expression and red vs. blue fill indicates higher expression. Heatmap: Scaled expression of T cell markers including costimulatory, activation, naive, exhaustion and regulatory T cell markers as well as AP1 signaling. Bottom: Proportion of cells in each cluster under stimulated vs. unstimulated conditions in sgCONT (blue) or sgIKZF2 (red) populations. Positive values indicate increase in cluster occupancy following stimulation. **E,** Expression of CXCL10 and CCND1 across clusters (violin plot). **F,** Expression of top upregulated genes in bulk RNA-seq for sgIKZF2 vs.

sgCONT across single cell clusters. **G** and **H,** Expression of IFNG(G) and CCL3(H) in sgCONT or sgIKZF2 CAR T-cells superimposed on the UMAP projection.

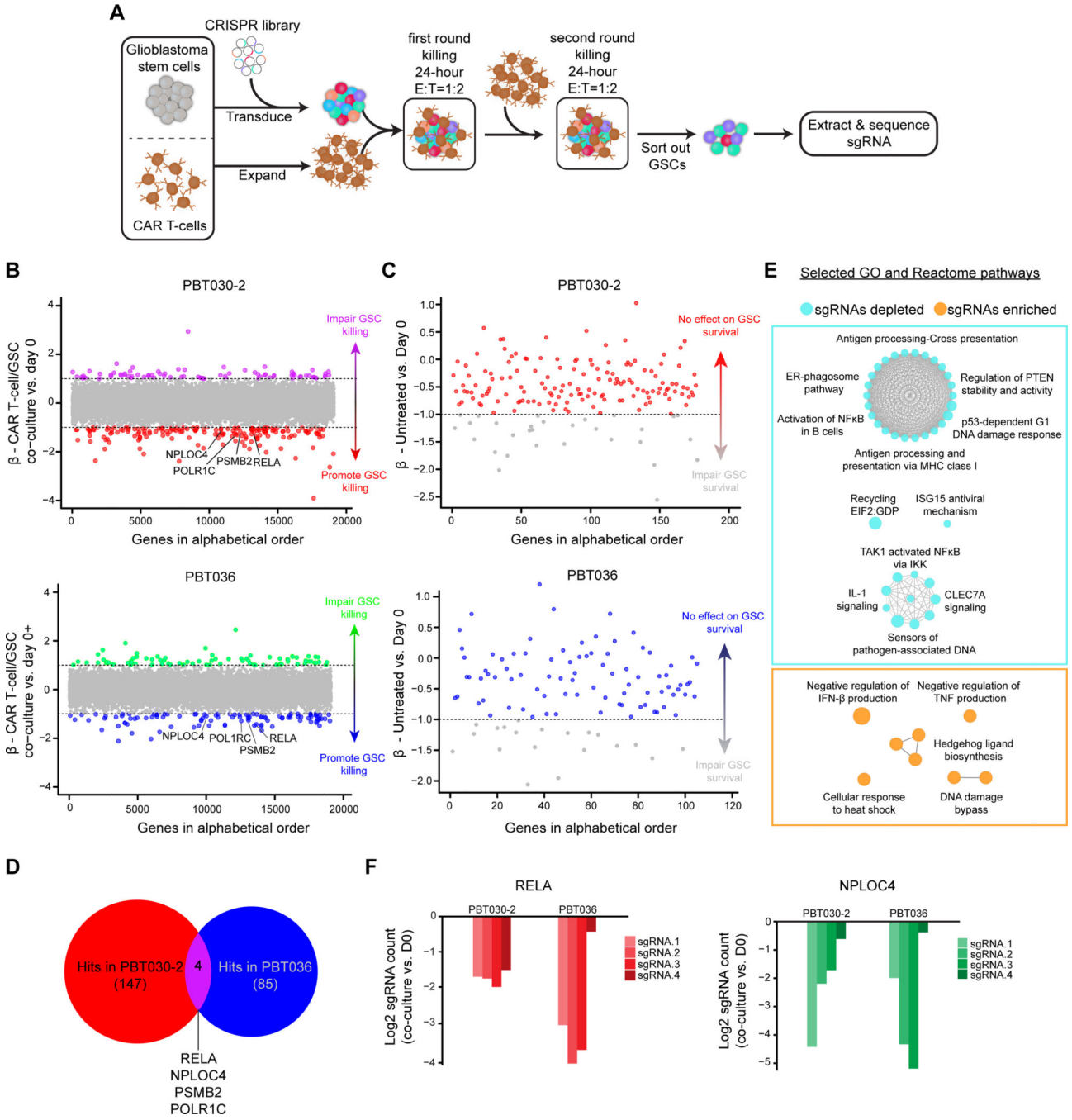

Figure 5. CRISPR-Cas9 screen in GSCs co-cultured with CAR T-cells.

A, Overview of screen design. GSCs were transduced with a whole-genome CRISPR-Cas9 library and subjected to two rounds of CAR T cell killing (total E:T=1:1). GSCs were then extracted, libraries were prepared, and sequenced to identify enriched and depleted guides. **B,** Results of the screen in each GSC model. Genes are ordered alphabetically on the x-axis and by MAGECK β score on the y-axis comparing co-culture vs. untreated GSCs. Genes in purple or green are enriched at $\beta > 1$ (sgRNAs targeting genes that impair GSC killing by CAR T-cells) and those in red or blue are depleted at $\beta < -1$ (sgRNAs targeting gene that

promote GSC killing by CAR T-cells). **C,** Plot of depleted genes for each model ordered alphabetically on the x-axis by MAGECK β score on the y-axis comparing untreated day ** vs. day 0. Points in grey are depleted at $\beta < -1$ (sgRNAs targeting the gene impair GSC survival). The remaining points in red or blue indicate genes for which knockout do not effect GSC survival. **D,** Venn diagram illustrating common hits for depleted genes in two models. **E,** ClueGO plot of GO and Reactome pathways enriched in the union of hits for both models. **F,** Log2 fold change of normalized counts for each sgRNA targeting common CRISPR screen hits comparing co-culture to day 0. GSC: glioblastoma stem cell.

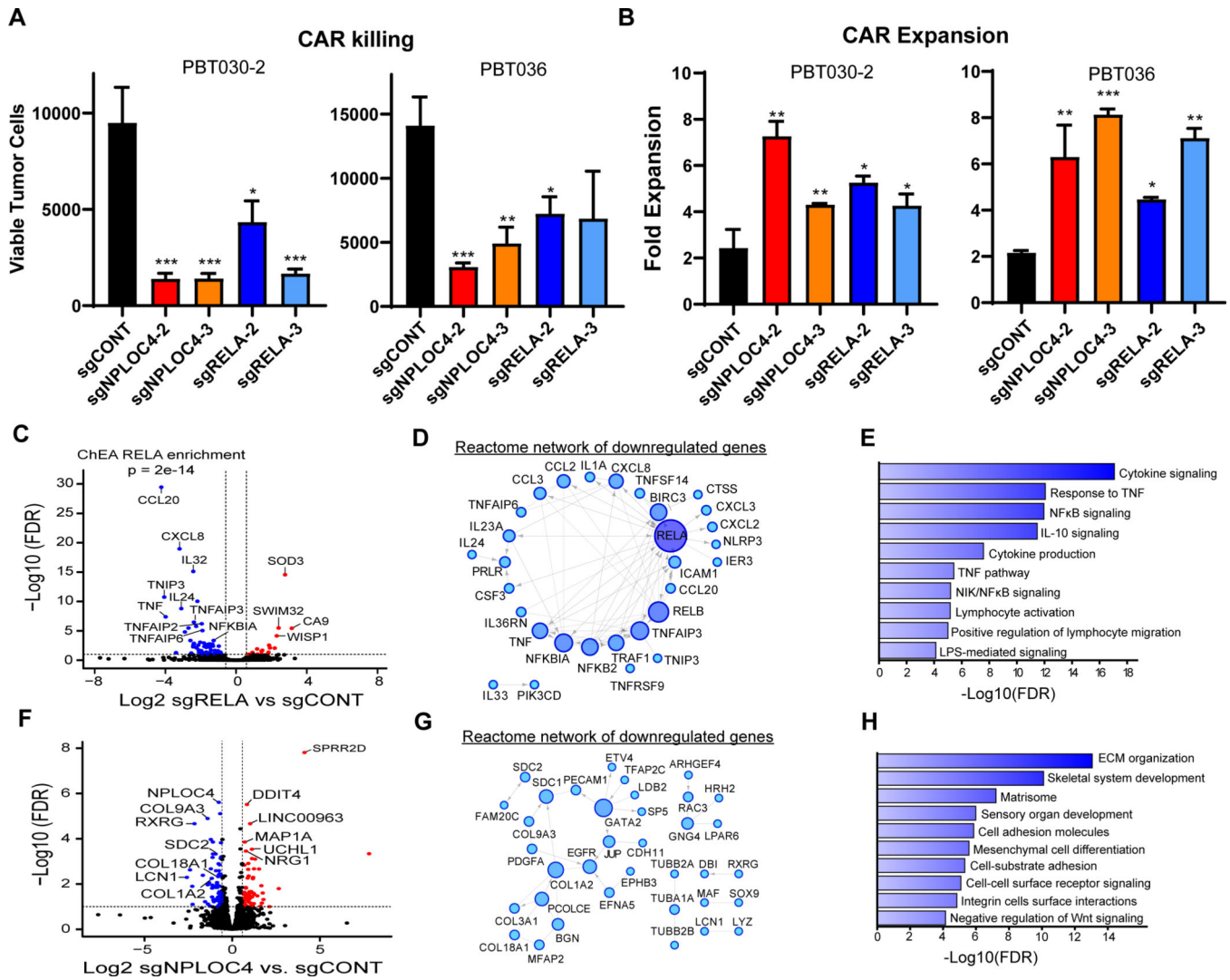

Figure 6. RELA or NPLOC4 disruption improves CAR T cell killing of GSCs.

A, CAR T cell killing of GSCs (E:T=1:40, 48 hours) with CRISPR-mediated knockout of RELA or NPLOC4. **B,** CAR T cell expansion in co-culture with GSCs (E:T=1:40, 48 hours) with CRISPR-mediated knockout of RELA or NPLOC4. (a, b) *p<0.05, **p<0.01, ***p<0.001 compared to GSCs transduced with non-targeting sgRNA (black) using unpaired Student's t tests. **C,** RNA-sequencing of GSCs following RELA knockout plotted as –log10 FDR (y-axis) vs. log2 fold change of RELA knockout vs. control (x-axis). Blue or red points are genes with <−1.5- or >1.5-fold change, respectively at an FDR of <0.05. **D,** Reactome network of genes downregulated following RELA knockout. Only genes linked in the Reactome database to at least one other gene are shown. Node size and color saturation are proportional to node degree. Activating interactions are indicated by arrowheads, while dotted lines indicate predicted interactions. **E,** Pathway enrichment of genes in the Reactome network of downregulated genes in (c). **F,** RNA-sequencing of GSCs following NPLOC4 knockout plotted as –log10 FDR (y-axis) vs. log2 fold change of NPLOC4 knockout vs. control (x-axis). Blue or red points are genes with <−1.5- or >1.5-fold change, respectively at an FDR of <0.05. **G,** Reactome network of genes downregulated

following NPLOC4 knockout. **H,** Pathway enrichment of genes in the Reactome network of downregulated genes in (F).

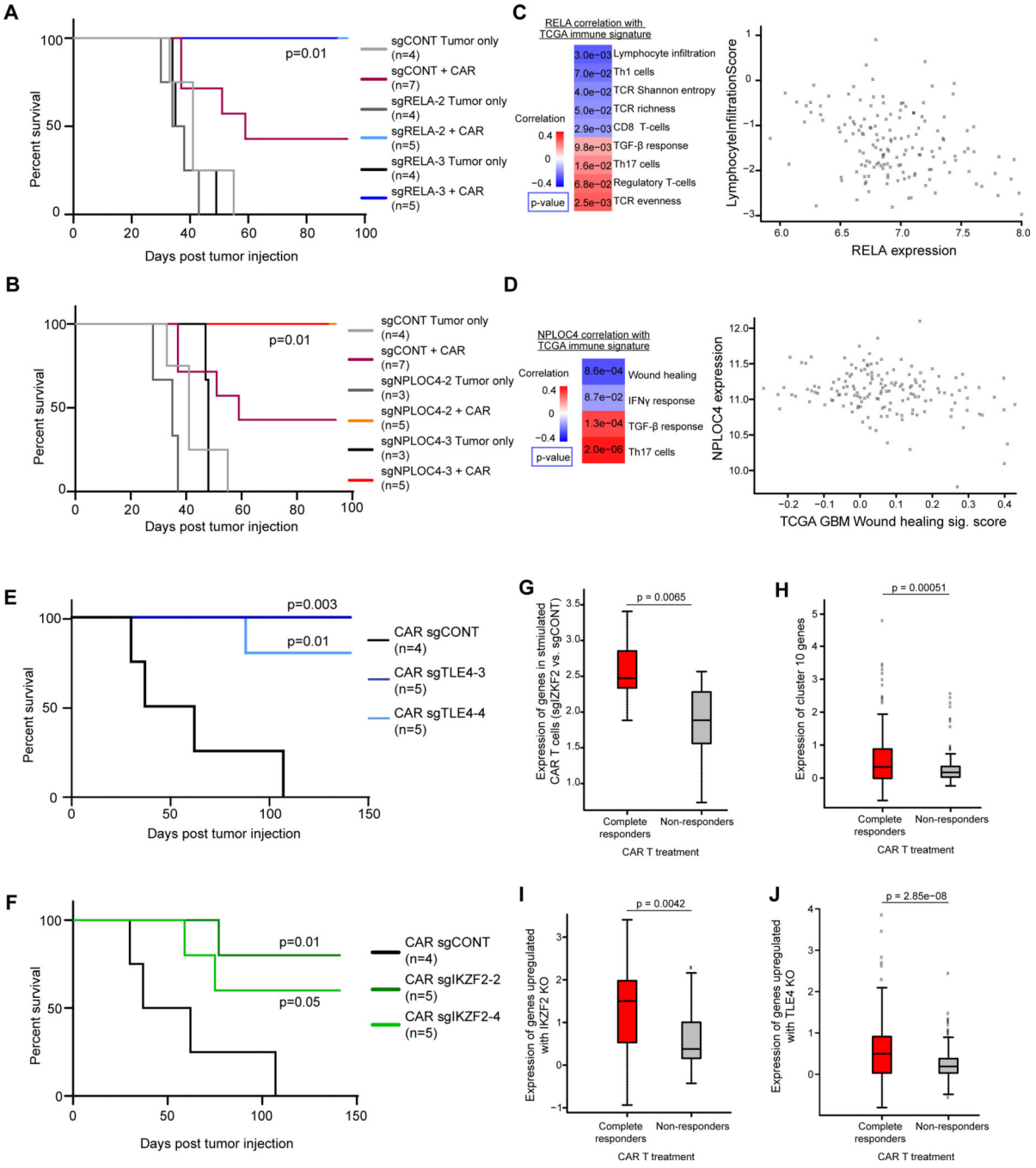

Figure 7. Functional and clinical relevance of targets on GSCs and CAR T cells.

A and **B,** Kaplan-Meier survival curves comparing mouse survival for RELA (A) or NPLOC4 (B) knockout with non-targeting controls. Tumors were established by orthotopically implanting 2×10^5 PBT030–2 GSCs, and treated after 8 days with 5×10^4 CAR T cells. P-values were shown comparing each group with “sgCONT+CAR” group using Log-rank test. **C,** Left: Correlation of RELA expression with immune and T cell signatures in TCGA GBM RNA-seq data. Right: Scatter plot of lymphocyte infiltration signature score vs. RELA expression by tumor from TCGA GBM RNA-seq data. **D,** Left:

Correlation of NPLOC4 expression with immune and T cell signatures in TCGA GBM RNA-seq data. Right: Scatter plot of NPLOC4 expression vs. wound healing signature score by tumor from TCGA GBM RNA-seq data. (C, D) p-values were calculated as Pearson's correlation coefficients. **E** and **F,** Kaplan Meier curves demonstrating prolonged survival in an intracranial xenograft model of GBM treated with TLE4KO (C) or IKZF2KO (D) CAR T-cells (blue) compared to non-targeting control (black). Tumors were established by orthotopically implanting 2×10^5 PBT030–2 GSCs, and treated after 8 days with 2×10^4 CAR T cells. P-values were shown comparing each group with the "CAR sgCONT" group using Log-rank test. FDR: False discovery rate. **G,** Fold change after stimulation of genes significantly upregulated (FDR < 0.05, Log2 fold change > 1) following IKZF2 knockout after tumor stimulation, in an independent dataset of clinical CAR T cells products from patients with CLL. **H,** Fold change after stimulation of genes enriched in cluster 10 as shown in Fig. 5. **I** and **J,** Fold change after stimulation of genes significantly upregulated (FDR < 0.05, Log2 fold change > 1) following IKZF2 (I) or TLE4 (J) knockout. (G-J) CAR T cells were stratified by response of the patient from which they were derived - complete responders or non-responders - to CAR therapy and the log2 fold change of stimulated vs. mock-stimulated gene expression was plotted, p-values were calculated by unpaired Student's t tests.